IEEE Access
Multidisciplinary | Rapid Review | Open Access Journal

Received 2 January 2024, accepted 6 January 2024, date of publication 10 January 2024,
date of current version 19 January 2024.

Digital Object Identifier 10.1109/ACCESS.2024.3352070

RESEARCH ARTICLE

Dynamics of Digital Pen-Tablet: Handwriting Analysis for Person Identification Using Machine and Deep Learning Techniques

TAHMID HASAN[1], MD. ABDUR RAHIM[1], JUNGPIL SHIN[2], (Senior Member, IEEE), SATOSHI NISHIMURA[2], (Member, IEEE), AND MD. NAJMUL HOSSAIN[3], (Member, IEEE)

[1]Department of Computer Science and Engineering, Pabna University of Science and Technology, Pabna 6600, Bangladesh
[2]School of Computer Science and Engineering, The University of Aizu, Aizuwakamatsu 965-8580, Japan
[3]Department of Electrical, Electronic and Communication Engineering, Pabna University of Science and Technology, Pabna 6600, Bangladesh

Corresponding authors: Jungpil Shin (jpshin@u-aizu.ac.jp) and Md. Abdur Rahim (rahim@pust.ac.bd)

This work was supported by the Competitive Research Fund of The University of Aizu, Japan.

ABSTRACT Handwriting is controlled by neurons in the brain's nervous system, reflecting an individual's personality and psychology. This unique characteristic can be used for various applications, including user authentication, assessment of neurodegenerative disorders, and classification of handedness, gender, and age groups. Traditional authentication systems require memorization, information leakage, and fingerprints, making them vulnerable to security breaches. The majority of researchers have studied the limitations of image quality, camera frames, and light effects on text and image-dependent performance. Therefore, this paper mainly focused on real-time, text-independent handwriting fine-motor data and proposed an efficient authentication system with low cost using efficient feature extraction and optimal feature selection approaches. This research utilizes two benchmark databases, including the handwriting data of 48 (24+24) participants collected via a sensor-based pen tablet. Each participant wrote the 10 words five times repeatedly, making it a total of 2400 samples. The handwriting classification of the different individuals is in 3 phases: feature extraction, feature selection, and classification. A total of 91 features (statistical, kinematic, spatial, and composite) were extracted from more accurate, real-time numerical handwriting data. The efficient and optimal features have been selected using four feature selection approaches, namely, Pearson's r correlation, ANOVA-F, Mutual Information Gain, and PCA, among which the ANOVA-F test and PCA perform well for handwriting-extracted data. Then, 14 machine learning (ML) models and 7 deep learning (DL) models were applied to handle the problem of individual classification, with both no- and full-feature-selection scenarios considered. The experimental analysis has been conducted with different angles and perspectives, such as K-Fold cross-validation, testing system efficiency considering 5/10/15/24/48 individuals, and in the case of individual tasks. It shows that ML-based algorithms, namely, CATBOOST (99.07%) with ANOVA-F and DL-based models, namely, BiLSTM (98.31%) with PCA-selected features, provide the highest accuracy with dataset 2, among others that advocate the practicality and reliability of choosing this system for user identification.

INDEX TERMS Digital pen-tablet, deep learning, feature extraction, handwriting analysis, machine learning, optimal feature selection, person identification.

I. INTRODUCTION

In the digital world, user authentication is essential in ensuring the security and protection of information, cybersecurity, the IoT (Internet of Things), network security, and web application security-based systems [1]. It restricts access to crucial assets, such as computing platforms, data stores, online gateways, and other interconnected applications, and ensures that only approved users can access sensitive information. This ensures the confidentiality and integrity of

The associate editor coordinating the review of this manuscript and approving it for publication was Jon Atli Benediktsson.

sensitive data in various industries, including finance, healthcare, and national security. Throughout history, numerous authentication techniques have emerged, each with its unique method of verifying identity. These techniques appropriately fall into three classes. a) those based on knowledge, b) reliant on tokens, and c) those utilizing biometrics [2]. Knowledge-based authentication methods, such as text passwords, are susceptible to password theft due to their reliance on a text password [3]. Token-based authentication provides a less arduous alternative to memorization, but token theft remains a concern [4]. Biometric-based systems, such as fingerprints, iris patterns, and facial recognition, offer a more secure solution with a lower risk of identity theft but face resistance from privacy-conscious users due to being traced [5]. Scholars in various fields have investigated user authentication methods utilizing various biometrics, including voice, DNA, iris patterns, hand geometry, fingerprints, keystroke dynamics, and more. Despite this, the unique and defining traits inherent in an individual's handwriting have been demonstrated to be a reliable means of authenticating a person offline and online [1].

In recent years, despite technological advancements and their ability to reveal unique properties and interconnection with the human brain, handwriting analysis has gained popularity among academics. Over the past two decades, numerous efforts have been made to utilize fine motor skills and patterns in one's handwriting for user identification and verification and to identify an individual's age group, gender, handedness, and mental state [6], [7]. With a handwriting recognition system, handwriting features are captured and analyzed through various inputs, including touch screens, electronic pens, images, pen tablets, scanners, and paper documents. Every person has a distinct handwriting style that makes it a compelling subject of study in user identification [8] and useful for various applications, such as personal identification [9], [10], pattern recognition, digital forensics, questioned document examination, criminalistics, fingerprint analysis, signature verification [11], [12], and biometric analysis [13]. Limited studies exist on the use of handwriting for user identification, with the majority of research focusing on using handwriting images to classify various factors such as age groups [14], nationality, age, and gender classification [15], handedness and gender [16], alcohol consumption detection [17], and Parkinson's disease [18]. In image-based studies, capturing the essence of a person's handwriting can be challenging with light and technology. Factors such as lighting, image encoding, brightness, camera specs, and image quality all contribute to capturing a clear image. Moreover, preprocessing to enhance the image adds complexity and computational cost. Image-based models ignore the essential features contained within the numerical values of a person's handwriting [1]. There is a lack of comprehensive studies that explore the potential of handwriting fine-motor features for person identification due to limitations in sample size, number of features, and feature selection approaches. Previous research has primarily relied on machine learning (ML)-based methods and has only tested a limited number of ML algorithms, and most of the works are text-dependent. Therefore, there is a need for further research to develop effective and accurate methods for person identification.

The main goal of this study is to find distinctive features in an individual's handwriting and provide a text-independent system for identifying users with near-perfect accuracy so that the obstacles imposed by the traditional system may be eliminated. To achieve this objective, using fine-motor numerical features of human handwriting collected by a digitized pen tablet sensor, several methodologies for feature extraction, feature selection techniques to extract and select relevant features, and machine learning (ML), deep learning (DL), and advanced hybrid model-based algorithms to classify users based on those features were applied. This paper utilizes 6-dimensional numeric, time-series pen tablet sensor data to analyze handwriting fine-motor skills. The dataset is analyzed to understand feature correlation and statistical distribution. Preprocessing is performed to prepare the data for input into the system, and a total of 91 statistical, kinematic, spatial, and composite features are extracted from the processed raw data. Optimal features are then selected from the extracted features using four selection approaches, as not all features contribute equally. For classification purposes, 14 machine-learning algorithms and 7 deep-learning approaches are experimented with for user authentication. This study conducts experiments on datasets encompassing diverse combinations and variations, including different numbers of individuals and task-specific accuracy levels. In this research study, our main contributions are:

- Conducting exploratory data analysis and preprocessing with various statistical approaches ensures the data is clean and ready for analysis.
- Using two different datasets and combining them to increase the generalizability of the results.
- Incorporating multiple techniques for efficient feature extraction from other scholars' work to improve the accuracy and diversity of features.
- Introducing 36 novel features to enhance user identification accuracy using handwriting.
- Experimenting with 4 different statistical feature selection approaches to identify the most important features for user identification.
- Offering a comprehensive investigation of user identification using time-series data on handwriting by employing 14 machine learning-based methods and 7 deep learning models.
- Proposing a novel hybrid deep learning architecture-a fusion comprising 'Time-Distributed BiGRU', 'BiLSTM', and 'CNN' for user identification using handwriting fine-motor features.

The remaining of this paper is organized as follows. Section II provides some works related to the influence of handwriting from different perspectives. Then, the materials

and proposed methods, including dataset preparation, data analysis and preprocessing, feature extraction, optimal feature selection process, and ML and DL classification model architectures, are explained briefly in Section III. The experimental results analysis and discussion are explained in Section IV. Finally, we give conclusions of this research work with future scope in Section V. Each section has necessary tables, figures, and charts to interpret and understand this research clearly.

II. LITERATURE REVIEW

A wealth of research has been conducted in the field of handwriting analysis, including the recognition of handwriting, diagnosis of developmental dysgraphia, detection of handedness, assessment of neurodegenerative diseases, signature verification, and identification of individuals based on image, pattern, fine motor traits, and gesture analysis. Our study focuses on identifying users through analyzing their handwriting time-series data and fine motor traits, where effective feature extraction and selection play a crucial role. Various theoretical and practical methods for image and pattern analysis-based handwriting recognition and person identification conducted by previous researchers are summarized in this section.

The study by Begum et al. [1] presents a user authentication system utilizing digital pen-tablet sensor data. An optimal feature selection model extracts statistical and kinematic features for user identification, with a hybrid filter-wrapper algorithm contributing to the system's 97% accuracy using SVM, LR, and RF classifiers. However, the study's database is limited and dynamic, and temporal and composite features still need to be explored, leaving room for improvement with larger datasets and incorporating deep learning algorithms. Dargan et al. [19] suggested a new way to identify users using the Devanagari script. The system would use pre-segmented characters and four different ways to get features: zoning, diagonal, transition, and peak extent-based features. The system utilized k-NN and linear SVM classifiers, achieving an identification accuracy of 91.53% when using zoning, transition, and peak extent-based features with a linear SVM classifier. Saini et al. [20] proposed a three-step approach to authenticate a mobile user based on keystroke dynamics in different positions. The model was optimized using Particle Swarm Optimization (PSO) and reduced the feature set by at least 50%. The best results were observed for the walking and relaxing positions, with a minimum equal error rate (EER) of 2.2%. Considering the user's emotional state and lowering the false rejection rate (FRR) could improve performance. The study did not consider typing positions such as standing and imposed no restrictions on hand posture during typing. Chen et al. [21] proposed a comprehensive mobile terminal browsing authentication method by combining three sub-models to achieve an average DR of 86% with a low WAR.

Nguyen et al. [22] investigated text-independent writer identification using an end-to-end deep-learning method. They utilized a Convolutional Neural Network (CNN) from image features and reported an accuracy of 91.8% in classifying 900 writers. A study by Javidi and Jampour [23] presented a deep learning system for offline text-independent writer identification. It combines deep and conventional features and employs a handwritten thickness descriptor auxiliary data (HTD) in a modified ResNet architecture. Future work could consider additional features and multimodal descriptions. In [24], a pre-trained Convolutional Neural Network (CNN) model called AlexNet was utilized to identify characters of the English and Arabic languages. The AlexNet architecture was used in its freeze form, where features were extracted from the ImageNet dataset and then transferred to the QUWI dataset for classification. The results showed that the approach had an accuracy of 88.11%. Baldominos et al. [25] introduced the use of CNNs in identifying handwritten characters, focusing on the difference between previous work that used data augmentation and the original dataset. They conducted a comprehensive and up-to-date review of the MNIIST and EMNIST datasets.

Recent studies have made significant progress exploring touchscreen gesture recognition in mobile devices during various tasks such as document reading, Virtual keyboard interactions, keystroke dynamics, web browsing, Complex typing patterns, and unstructured tasks [26], [27], [28]. In the field of writer identification, a range of techniques has been explored, including Support Vector Machines [29], [30], distance-based methods [31], [32], and deep learning techniques [33]. The methods employed for writer identification are diverse and varied. Research from references [34], [35], [36], [37], and [38] focused on handwriting recognition and personal identification, utilizing image and pattern analysis. However, these systems come with a high computational cost.

The study of handwriting fine motor features has gained significant attention in recent years, with various research efforts focused on tasks such as Archimedean spiral tracing, letter writing, word writing, sentence writing, and loop drawing [39], [40], [41]. Moetesum et al. [39] investigated the potential of handwriting visual attributes in predicting Parkinson's disease in 72 subjects with an accuracy of 83% using SVM. Using Convolutional Neural Networks, static visual attributes were extracted, and median residual, edge images, and raw images were used to enrich the feature set. The study lacks a combined evaluation of offline features with other online features to predict PD and other neurological diseases. The potential of other drawing tasks also remains unexplored. The approach for calculating kinematic features in the handwriting of Parkinson's disease(PD) patients was proposed by Mucha et al. [40]. The fractional derivatives have been applied to the data of 30 PD patients and 36 healthy controls. The classification was performed using support vector machines and random forests, improving accuracy by 8% in univariate analysis and 10% in multivariate analysis. However, the limitations of this study include a need for more investigation into the use of temporal, spatial, and dynamic features.

The Impedovo et al. study presented a methodology for the early-stage diagnosis of Parkinson's disease using dynamic features of handwriting and motor skills [41]. The research used the publicly available PaHaW dataset and an ML classifier-based classification framework with an ensemble scheme achieving an accuracy of 74.76%. The study's limitations include the need for a larger benchmark dataset, combining dynamic and static handwriting features, and the potential to gain novel insights by considering other kinematic properties of human motor control as features.

III. MATERIALS AND METHODS

The summary of the proposed ML-based and DL-based frameworks is outlined in this section. Two benchmark datasets are used in this investigation. Furthermore, data analysis and preprocessing, feature extraction, feature selection, dimension reduction, ML classification models, DL architectures, and various evolution metrics have been emphasized.

A. PROPOSED METHOD

This study proposes a system paradigm for writer/person/user identification using an ML-based model and Deep Neural Network approaches based on their handwriting time-series features. The approach for handwriting analysis is pen-tablet-based and relies on extracting features from time-series signals associated with handwriting movements during handwriting tasks (i.e., x-y coordinate, pressure, angle, timestamp, azimuth, and altitude). However, several phases make up the proposed system: data description and acquisition process, exploratory data analysis, data preprocessing, feature extraction, train-test-classify with all features, optimal feature selection and classification, and performance assessment based on various combinations of datasets (for example, individual task-wise classification, individual user identification, 5/10/15/20/24/48 persons categorization). The functional flow and the interconnection of components of the proposed system are depicted in Fig. 1.

B. DATASET

Many data-collection devices are now available as a consequence of recent technological advances. The digital pen tablet is frequently used to observe dynamic handwriting characteristics [42]. However, the datasets acquired by [1] and [43], used a digitized graphics tablet. The major concern of a sensor error on the tablet surface and pen might appear in various ways, including random, small, and unwanted movement of the pointer or pen tip on the tablet surface. Furthermore, the calibration problem with the tablet causes the pen input to be imperceptible or less sensitive. This requires the tablet to align the pen input with the screen cursor properly. Furthermore, there is a visible gap between the pen tip and the actual location on the screen; therefore, pressure sensitivity sensor problems may result in inconsistent line thickness. However, the author collected data using a Wacom Intuos Pro digitizing tablet with a wireless pen and a pressure-sensitive tip capable of precisely capturing all kinematic, temporal, and pressure data without any concerning mistakes. Both datasets have identical characteristics/parameters. The dataset contains numerous handwritten samples from 24 (Dataset 1) and 24 (Dataset 2) male and female individuals aged 19 to 40 making 1,464,547 records/rows. Each individual performed a total of ten tasks each five times. The lengths of the tasks vary, making the dataset more robust and diversified. The tasks include the words are: ''Japan'', ''Machine Learning'', ''Tokyo'', ''Hello world'', ''Fukushima'', ''Aizu University'', ''Basic Research'', ''Computer Vision'', ''Pattern Processing'', and ''Thank You'' and labelled as Task 1, Task 2, Task 3 $\cdots$ Task 10. We incorporated both datasets and performed a complete and in-depth analysis of user identification using six time-series features. Table 1 presents the overall characteristics of the benchmark datasets. Six-dimensional time series features, namely ''Writing Time'', ''X-axis'', ''Y-axis'', ''Pen Pressure'', ''Horizontal Angle'', and ''Vertical Angle'' have been obtained from pen tablets, which are visually illustrated in Fig. 2 [44].

C. PREPROCESSING OF RAW TIME-SERIES DATASET

Preprocessing Six-dimensional raw data is essential for handwriting recognition, as it eliminates interference caused by technological limitations [45]. Our methodology utilizes the nearly pristine on-surface data for feature computation [1], requiring minimal data preparation. This study uses several preprocessing techniques to attain a more harmonious dataset and enhance performance.

1) OUTLIER DETECTION AND REMOVAL

An outlier can be defined as a solitary data point that diverges notably from the rest of the dataset or observations. Outliers can significantly impact statistical procedures, leading to inaccurate and untrustworthy outcomes. We used both box-whisker plots and bell curves as analytical tools to identify outliers, and to remove outliers from our dataset, we employed two methods - the z-score approach and the quartile (percentile) approach.

Z Score Approach The Z-score is a metric that quantifies the degree of deviation of an experimental result from the mean [46]. The Z-score is calculated by Equation (1).

$$Z = \frac{X - \mu}{\sigma} \tag{1}$$

where μ defines the mean and σ standard deviation.

Percentile (Quartile) Approach Quartiles are a statistical measure that splits the data into four equal parts, dividing the data points into quarters. They are calculated by sorting the data in ascending or descending order and then looking at the middle 25% or the bottom 25%, thus making them a type of order statistic [47]. The present investigation adopted a lower and upper boundary threshold of 0.07 and 0.95, respectively. The first quartile of the dataset is denoted as Quartile 1 ($Q1$), whereas the third quartile as Quartile 3 ($Q3$). We utilized

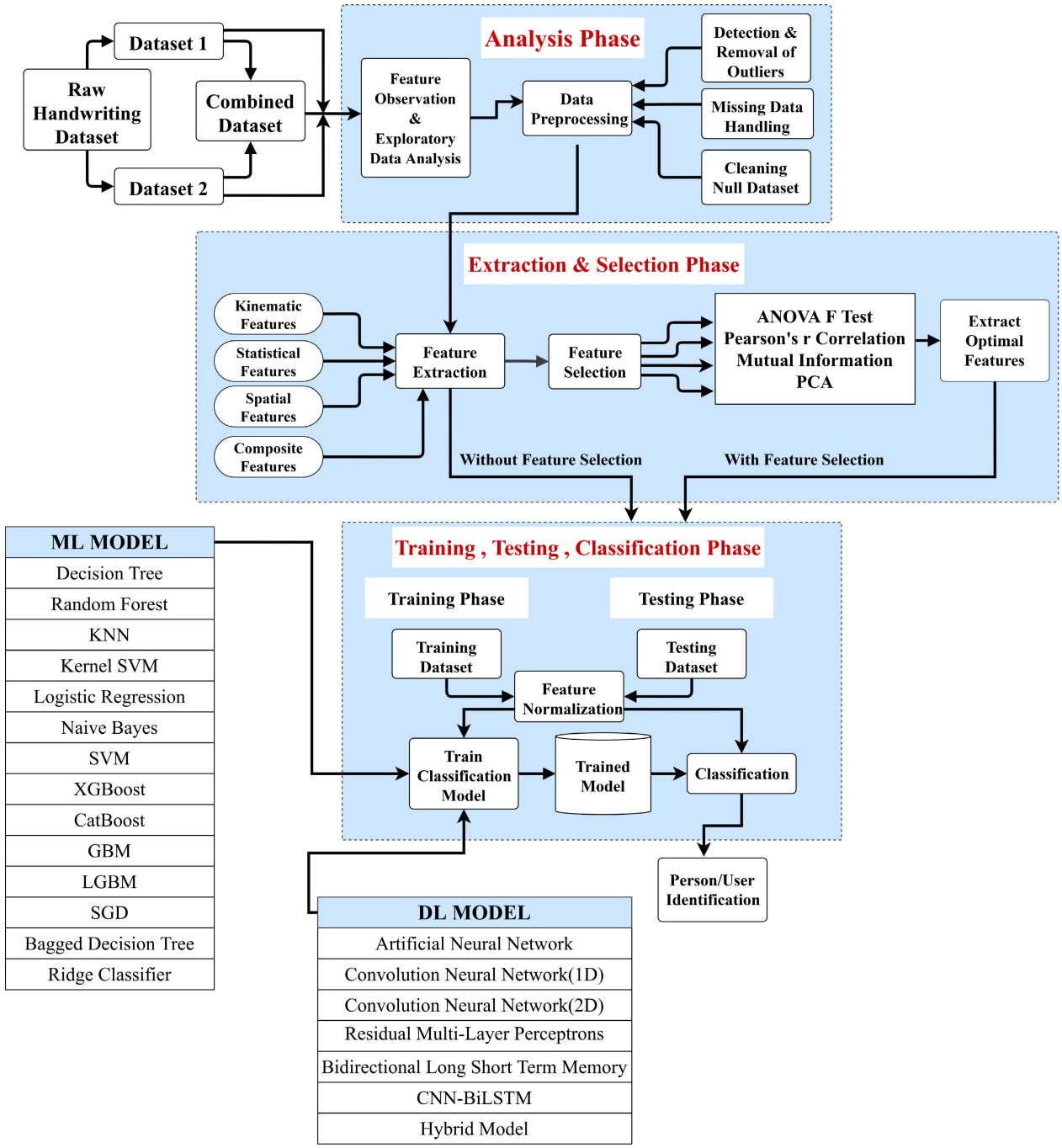

FIGURE 1. General workflow of the proposed person identification system.

percentile techniques for detecting outliers by the following steps:

- Calculation of the Interquartile Range (IQR).
- The IQR is calculated by subtracting the first ($Q1$) quartile from the third ($Q3$); IQR = $Q3$-Q.
- Establishing the lower boundary by subtracting 1.5 times the IQR from $Q1$; Lower Boundary = $Q1$ - 1.5×IQR.
- Setting the upper Boundary by adding 1.5 times the IQR to $Q3$; Upper Boundary = $Q3$ + 1.5× IQR.

The quartile-percentile technique was applied to the two databases, comprising 2400 records stored in CSV files.

2) HANDLING MISSING VALUES

Unfortunately, some of the values in the dataset are missing, likely due to fluctuations in the timing discrepancies between data capturing and acquiring devices, causing lost signals and null values. Thus, the imputation function replaced the missing values [1], ensuring that all column attributes contain

TABLE 1. Summary of the overall characteristics of the handwriting dataset.

Database	No. of Subjects	Age (years)	No. of Words	Total Sample/ Files(.csv)	No. of rows/records in each file		
					Maximum	Minimum	Total
Dataset 1	24	19 ∼ 40	10 (5 iterations)	1200 (50 × 24)	3668	318	773660
Dataset 2	24	19 ∼ 40	10 (5 iterations)	1200 (50 × 24)	1838	47	690887
Combined	48	19 ∼ 40	10 (5 iterations) (50 × 48)	2400	-	-	1464547

TABLE 2. Interpretation and mathematical formulation of statistical features.

Features	Statistical Function	Description	Equation/Formula
Pen Pressure	Mean	Average of parameters extracted from signals at each timestamp during the writing	$\bar{X} = \frac{\sum_{i=1}^{n} X_i}{n}$
X-Coordinate	Median	A median of parameters collected from signals at each timestamp during the writing	$M = (\frac{\frac{n}{2} - cf}{f})(w) + L_m$
Y-Coordinate	Maximum	Maximum of parameters extracted from signals at each timestamp during the writing	$\text{MAX}(X_1, X_2, X_3, \ldots, X_n)$
Horizontal Angle	Minimum	Minimum of parameters collected from signals at each timestamp during the writing	$\text{MIN}(X_1, X_2, X_3, \ldots, X_n)$
Vertical Angle	Variance	The variance of parameters extracted from signals at each time stamp during the writing	$\sigma_n = \sqrt{\frac{1}{n}\sum_{i=1}^{n}(X_i - \bar{X})^2}$
	Standard Deviation	The std of parameters extracted from signals at each time stamp during the writing	$\sigma(\text{std}) = \sqrt{\frac{1}{N-1}\sum_{i=1}^{N}(X_i - \bar{X})^2}$

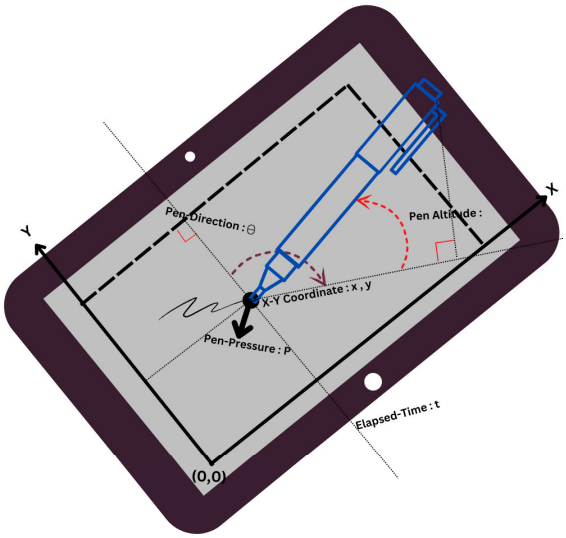

FIGURE 2. Handwriting 6-Dimensional Data Description using pen-tablet Device.

valid numerical values. The method chosen for this study was mean imputation, in which the missing values were filled with the mean value of the corresponding attribute in the dataset. The formula employed for the mean imputation of a column in the dataset is expressed as follows by Equation (2).

$$\frac{\sum_{i=0}^{N} f_i}{N} \tag{2}$$

The variable f_i denotes the frequency of instances within a given column where imputation has been applied, and N is the total number of cases in a feature vector.

D. FEATURE EXTRACTION

In this research, Feature Extraction is of utmost significance in identifying users, as the raw time series data lack distinct features per individual. Writer identification relies heavily on the accuracy of feature extraction and selection. Hence, extracting features from the 6-dimensional raw time-series data is significant to differentiate between individuals. This study draws up two databases containing 2400 CSV files, equally divided into two collections with 1200 files each, to gather features for identifying 48 subjects (24 class+24 class). From the raw time-series dataset, 91 features were extracted. These included 25 statistical features [1], [7], [48], 12 kinematic features [1], [7], [48], [49], 15 composite features [8], and 39 spatial features, 36 of which were new and created through complicated mathematical calculations [46]. The statistical, kinematic, spatial, and composite features are represented in Table 2, Table 3, Table 4, and Table 5, respectively.

E. FEATURE SELECTION

When working with high-dimensional data, a barrier can be encountered that may be alleviated by feature selection. By removing redundant and irrelevant data, feature selection can improve computation efficiency, enhance learning accuracy, and deepen the model's capability [50]. An abundance of features (91 features) was generated during the feature extraction phase, leading to the "curse of dimensionality," as first discussed by Bellman [51], which decreases the accuracy and reliability of classification and prolongs the learning process. The contribution of each feature towards accurately predicting the target class is of varying degrees. whereas

TABLE 3. Interpretation and mathematical formulation of kinematic features.

Features	Statistical Function	Equation/Formula	Description
Pressure	Average	$\text{Pressure}_{\text{mean}} = \frac{1}{N} * \sum_{n=1}^{N}(P_n)$	Pen tip pressure averaging over all pressures at the specified timestamps
	Peak Pressure	$\text{Pressure}_{\text{peak}} = 1 \leq N_{\max}(P_n)$	Maximum pressure within the writing period
Writing Speed	Average	$\text{Speed}_{\text{avg}} = \frac{1}{N}\sum_{n=1}^{N}\frac{\sqrt{(X_{n+1}-X_n)^2+(Y_{n+1}-Y_n)^2}}{\text{time}_{n+1}-\text{time}_n}$	Average velocity within the specified timestamp
	Standard Deviation	$\text{Speed}_{\sigma} = \sqrt{\frac{1}{n-1}\sum_{i=1}^{n}(V_i-\bar{V})^2}$	Std. of velocities within the provided timestamp
	Peak Speed	$\text{Velocity}_{\text{peak}} = \max_{1\leq n\leq N}\frac{\sqrt{(X_n-X_{n+1})^2+(Y_n-Y_{n+1})^2}}{\text{time}_{n+1}-\text{time}_n}$	Maximum speed within the writing period
	Minimum	$\text{MIN}(V_1, V_2, V_3, \ldots, V_n) > 0$	Minimum velocity non-zero value within the writing period
Velocity	Horizontal	$\text{Velocity}_h = \sum_{n=1}^{N}\frac{X(axis)_{n+1}-X(axis)_n}{\text{time}_{n+1}-\text{time}_n}$	Velocity along the horizontal axis
	Vertical	$\text{Velocity}_v = \sum_{n=1}^{N}\frac{Y(axis)_{n+1}-Y(axis)_n}{\text{time}_{n+1}-\text{time}_n}$	Velocity along the vertical axis
Acceleration	Average	$\text{Acc}_{\text{avg}} = \frac{1}{N}\frac{\sqrt{(X_{n+1}-X_n)^2+(Y_{n+1}-Y_n)^2}}{(\text{time}_{n+1}-\text{time}_n)^2}$	Average Rate of change in velocities within the period of writing
	Standard Deviation	$\text{Acc}_{\sigma} = \sqrt{\frac{1}{n-1}\sum_{i=1}^{n}(a_i-\bar{a})^2}$	Std. of acceleration
	Peak Acc.	$\text{MAX}(\frac{\triangle v}{\triangle t})$	Peak rate of change in velocities
	Minimum	$\text{MIN}(a_1, a_2, a_3, \ldots, a_n) > 0$	Minimum non-zero acceleration value within the writing period

some features possess considerable predictive characteristics, others exhibit limited or no ability.

1) FEATURE SELECTION TECHNIQUES

This study employs various methods for selecting the most relevant features for classification purposes. The feature selection techniques applied include

a) Pearson's r Correlation
b) One-way analysis of variance (ANOVA F test)
c) Mutual Information Score (MI)
d) Principal Component Analysis (PCA)

a: PEARSON'S R CORRELATION

Pearson's Correlation coefficient measures the direct relationship between two variables based on their covariance. Bonett et al. observe that Spearman's correlation coefficient is more volatile than Pearson's, implying that it is less reliable [52]. The Pearson r correlation is generated using Equation (3) [53].

$$r_{xy} = \frac{n\sum x_i y_i - \sum x_i \sum y_i}{\sqrt{n\sum x_i^2 - (\sum x_i)^2}\sqrt{n\sum y_i^2 - (\sum y_i)^2}} \tag{3}$$

where, r_{xy}, Pearson r correlation coefficient (r_{xy}) between variables x and y, n represents the total number of observations, x_i denotes the value of x for the ith observation, and y_i denotes the value of y for the ith observation.

b: ANOVA-F STATISTIC TEST

As per Hartung et al. [54], the ANOVA F-test can evaluate group variation for values other than zero. In utilizing this approach on the extracted handwriting features, the feature parameters can be assessed to determine if there is any variability among individuals. The process of conducting a one-way analysis of variance is outlined below [44].

Assuming that there are m distinct groups, a total of r cases, r_j cases per group, $\bar{X}$ represents the average of all issues, and $\bar{X}_j$ signifies the average of each group $\bar{X}_j$ ($j = 1, 2, \ldots, m$).
I. Compute the between-group sum of squares S_{btg} using Equation (4), where *btw* indicates "between groups".

$$s_{btg} = \sum_{i=1}^{m} r(\bar{X}_j - \bar{X})^2 \tag{4}$$

II. Calculate the sum of squares S_{wtg} using Equation (5), where *wtg* indicates "within the group".

$$s_{wtg} = \sum_{i=1}^{m}\sum_{i=1}^{r_j}(X_{ij} - \bar{X}_j)^2 \tag{5}$$

III. Determine dgf_b and dgf_w, the degrees of freedom using Equation (6) and Equation (7).

$$\text{dgf}_b = m - 1 \tag{6}$$

$$\text{dgf}_w = r - m \tag{7}$$

TABLE 4. Interpretation and mathematical formulation of spatial features.

SN	Features	Statistical Function	Description	Equation/Formula
1	Handwriting Width	...	From the starting of the X-coordinate until the end of the X-coordinate	MAX(X)-MIN(X) [1]
2	Handwriting Height	...	Distance from the top to the bottom	MAX(Y)-MIN(Y) [1]
3	Total Length	...	Total distance covered during the writing	$L = \sum_{i=1}^{N} \sqrt{(X_{i+1} - X_i)^2 + (Y_{i+1} - Y_i)^2}$
4	Pressure at the starting position	avg.	Mean pressure at the starting point	$P_{\text{start(avg)}} = \frac{1}{N} * \sum_{n=1}^{N} \text{MIN}(X) P_n$
5		Max.	Max. pressure at the starting point	$P_{\text{start(max)}} = \max[\sum_{n=1}^{N} \text{MIN}(X) P_n]$
6		Min.	Min. pressure at the starting point	$P_{\text{start(min)}} = \min[\sum_{n=1}^{N} \text{MIN}(X) P_n]$
7	Horizontal Angle at the starting position	avg.	Mean horizontal at the starting point	$H_{\text{start(avg)}} = \frac{1}{N} * \sum_{n=1}^{N} \text{MIN}(X) H_n$
8		Max.	Max. horizontal at the starting point	$H_{\text{start(max)}} = \max[\sum_{n=1}^{N} \text{MIN}(X) H_n]$
9		Min.	Min. horizontal at the starting point	$H_{\text{start(min)}} = \min[\sum_{n=1}^{N} \text{MIN}(X) V_n]$
10	Vertical Angle at the start time of writing	avg.	Mean vertical the angle at the starting point	$V_{\text{start(avg)}} = \frac{1}{N} * \sum_{n=1}^{N} \text{MIN}(X) H_n$
11		Max.	Max. vertical the angle at the starting point	$V_{\text{start(max)}} = \max[\sum_{n=1}^{N} \text{MIN}(X) H_n]$
12		Min.	Min. vertical angle at the starting point	$V_{\text{start(min)}} = \min[\sum_{n=1}^{N} \text{MIN}(X) V_n]$
13	Pressure at the ending position	avg.	Mean pressure at the ending point	$P_{\text{end(avg)}} = \frac{1}{N} * \sum_{n=1}^{N} \text{MAX}(X) P_n$
14		Max.	Max. pressure at the ending point	$P_{\text{end(max)}} = \max[\sum_{n=1}^{N} \text{MAX}(X) P_n]$
15		Min.	Min. pressure at the ending point	$P_{\text{end(min)}} = \min[\sum_{n=1}^{N} \text{MAX}(X) P_n]$
16	Horizontal Angle at the ending position	avg.	Mean hor. angle at the ending point	$H_{\text{end(avg)}} = \frac{1}{N} * \sum_{n=1}^{N} \text{MAX}(X) H_n$
17		Max.	Max. hor. angle at the ending point	$H_{\text{end(max)}} = \max[\sum_{n=1}^{N} \text{MAX}(X) H_n]$
18		Min.	Min. hor. angle at the ending point	$H_{\text{end(min)}} = \min[\sum_{n=1}^{N} \text{MAX}(X) V_n]$
19	Vertical Angle at the ending time of writing	avg.	Mean ver. angle at the ending point	$V_{\text{end(avg)}} = \frac{1}{N} * \sum_{n=1}^{N} \text{MAX}(X) H_n$
20		Max.	Max. ver. angle at the ending point	$V_{\text{end(max)}} = \max[\sum_{n=1}^{N} \text{MAX}(X) H_n]$
21		Min.	Min. hor. angle at the ending point	$V_{\text{end(min)}} = \min[\sum_{n=1}^{N} \text{MAX}(X) V_n]$
22	Pressure at the peak/top position	avg.	Mean pressure at the peak point	$P_{\text{peak(avg)}} = \frac{1}{N} * \sum_{n=1}^{N} \text{MAX}(Y)(P_n)$
23		Max.	Max. pressure at the peak point	$P_{\text{peak(max)}} = \max[\sum_{n=1}^{N} \text{MAX}(Y)(P_n)]$
24		Min.	Min. pressure at the peak point	$P_{\text{peak(min)}} = \min[\sum_{n=1}^{N} \text{MAX}(Y)(P_n)]$
25	Horizontal Angle at the peak position	avg.	Mean hor. angle at the peak point	$H_{\text{peak(avg)}} = \frac{1}{N} * \sum_{n=1}^{N} \text{MAX}(Y)(H_n)$
26		Max.	Max. hor. angle at the peak point	$H_{\text{peak(max)}} = \max[\sum_{n=1}^{N} \text{MAX}(Y)(H_n)]$
27		Min.	Min. hor. angle at the peak point	$H_{\text{peak(min)}} = \min[\sum_{n=1}^{N} \text{MAX}(Y) V_n]$
28	Vertical Angle at the peak position	avg.	Mean ver. angle at the peak point	$V_{\text{peak(avg)}} = \frac{1}{N} * \sum_{n=1}^{N} \text{MAX}(Y) H_n$
29		Max.	Max. ver. angle at the peak point	$V_{\text{peak(max)}} = \max[\sum_{n=1}^{N} \text{MAX}(Y)(H_n)]$
30		Min.	Min. hor. angle at the peak point	$V_{\text{peak(min)}} = \min[\sum_{n=1}^{N} \text{MAX}(Y) V_n]$
31	Pressure at the bottom position	avg.	Mean pressure at the bottom point	$P_{\text{bottom(avg)}} = \frac{1}{N} * [\sum_{n=1}^{N} \text{MIN}(Y)(P_n)]$
32		Max.	Max. pressure at the bottom point	$P_{\text{bottom(max)}} = \max[\sum_{n=1}^{N} \text{MIN}(Y)(P_n)]$
33		Min.	Min. pressure at the bottom point	$P_{\text{bottom(min)}} = \min[\sum_{n=1}^{N} \text{MIN}(Y) P_n]$
34	Horizontal Angle at the bottom position	avg.	Mean hor. angle at the bottom point	$H_{\text{bottom(avg)}} = \frac{1}{N} * [\sum_{n=1}^{N} \text{MIN}(Y) H_n]$
35		Max.	Max. hor. angle at the bottom point	$H_{\text{bottom(max)}} = \max[\sum_{n=1}^{N} \text{MIN}(Y) H_n]$
36		Min.	Min. hor. angle at the bottom point	$H_{\text{bottom(min)}} = \min[\sum_{n=1}^{N} \text{MIN}(Y) V_n]$
37	Vertical Angle at the bottom position	avg.	Mean ver. angle at the bottom point	$V_{\text{bottom(avg)}} = \frac{1}{N} * [\sum_{n=1}^{N} \text{MIN}(Y) H_n]$
38		Max.	Max. ver. angle at the bottom point	$V_{\text{bottom(max)}} = \max[\sum_{n=1}^{N} \text{MIN}(Y) H_n]$
39		Min.	Min. hor. angle at the bottom point	$V_{\text{bottom(min)}} = \min[\sum_{n=1}^{N} \text{MIN}(Y) V_n]$

IV. Determine the unbiased variances Var_b and Var_w using Equation (8) and Equation (9).

$$\text{Var}_b = \frac{S_{\text{btg}}}{\text{dgf}_b} \tag{8}$$

$$\text{Var}_w = \frac{S_{\text{wtg}}}{\text{dgf}_w} \tag{9}$$

V. Compute ANOVA F-value F using Equation (10).

$$\text{Anova}, F = \frac{\text{Var}_b}{\text{Var}_w} \tag{10}$$

The variance both within and between groups has an impact on the F-value, which quantifies the degree of differentiation.

c: MUTUAL INFORMATION SCORE

The entropy loss is measured regarding target values using mutual information (MI). The range of MI scores is 0 to ∞. A high value of MI indicates a close relationship between the feature and the target, emphasizing the significance of the feature for model training [55]. The mutual information

TABLE 5. Interpretation and mathematical formulation of composite features.

SN	Features	Statistical Function	Description	Calculated Formula
1	Positive Pressure Change	Mean	Mean, Max and Std. of the rate of pressure change in a positive direction	$\frac{1}{N} \times \sum_{i=1}^{N} \frac{P_{k+1}-P_k}{t_{k+1}-t_k}; P_{k+1} > P_k$
2		Std.		$\text{Std}[\frac{P_{k+1}-P_k}{t_{k+1}-t_k}]; P_{k+1} > P_k$
3		Max		$\text{MAX}[\frac{P_{k+1}-P_k}{t_{k+1}-t_k}]; P_{k+1} > P_k$
4	Pressure Change in Negative Direction	Mean	Mean, Max and Std. of the rate of pressure change in a negative direction	$\frac{1}{N} \times \sum_{k=1}^{N} \frac{P_{k+1}-P_k}{t_{k+1}-t_k}; P_k > P_{k+1}$
5		Std.		$\text{Std}[\frac{P_{k+1}-P_k}{t_{k+1}-t_k}]; P_k > P_{k+1}$
6		Max.		$\text{MAX}[\frac{P_{k+1}-P_k}{t_{k+1}-t_k}]; P_k > P_{k+1}$
7	The first 10% of pen pressure	Mean	Standard Deviation and mean of pressure recorded in the first 10% sample	$P_{m(1st)} = \frac{1}{L} \times \sum_{n=1}^{L} P(n); L = \frac{N(\text{total } P)}{10}$
8		Std.		$P_\sigma = \sqrt{\frac{1}{k-1} \sum_{i=1}^{i=k} (P_i - \overline{P})^2}; k = \frac{N(total\ P)}{10}$
9	The last 10% of pen pressure	Mean	Mean and Standard Deviation of pressure recorded in the last 10% sample	$P_{m(last)} = \frac{1}{L} \times \sum_{n=1}^{L} P(n); L = \frac{9 \times N(\text{total } P)}{10}$
10		Std.		$P_{\sigma(last)} = \sqrt{\frac{1}{k-1} \sum_{i=1}^{i=k} (P_i - \overline{P})^2}; k = \frac{9 \times N(total\ P)}{10}$
11	First 10% of writing speed	Mean	Mean and Standard Deviation of velocity recorded in the first 10% sample	$\text{Speed}_{m(1st)} = \frac{1}{k} \sum_{n=1}^{k} \frac{\sqrt{(X_{n+1}-X_n)^2+(Y_{n+1}-y_n)^2}}{time_{n+1}-time_n}; k = \frac{N(\text{total speed})}{10}$
12		Std.		$S_\sigma = \sqrt{\frac{1}{k-1} \sum_{i=1}^{i=k} (S_i - \overline{S})^2}; k = \frac{N(\text{total speed})}{10}$
13	The last 10% of writing speed	Mean	Mean and Standard Deviation of velocity recorded in the last 10% sample	$\text{Speed}_{m(last)} = \frac{1}{k} \sum_{n=1}^{k} \frac{\sqrt{(X_{n+1}-X_n)^2+(Y_{n+1}-y_n)^2}}{t_{n+1}-t_n}; k = \frac{9 \times N(\text{total speed})}{10}$
14		std.		$S_\sigma = \sqrt{\frac{1}{k-1} \sum_{i=1}^{i=k} (S_i - \overline{S})^2}; k = \frac{9 \times N(\text{total speed})}{10}$
15	Loop Count	...	The period spent writing on the tablet surface is divided by the number of maxima	$\frac{\max(t)-\min(t)}{\text{length}(\max(y))}$

between two random variables, Variable1 and Variable2, is calculated [56] using Equation (11) as follows:

$$I(Variable1; Variable2) = H(Variable1) - H(Variable1|Variable2) \quad (11)$$

where H(Variable1) represents the entropy of Variable1 and H (Variable1 | Variable2) represents the conditional entropy of Variable1 given Variable2. The resulting I(Variable1; Variable2) value represents the mutual information between *Variable*1 and *Variable*2, expressed in bit units.

Implementation Process (ANOVA + MI) This experiment used only dataset 1 to perform an ANOVA-F and MI test. All 91 features from dataset 1 were tested against these two methods, and the features were ranked in decreasing priority and from most important to least important. The proposed approach analyzes the logistic regression model's classification accuracy by gradually integrating the features in decreasing order of importance. The steps involved are:

- Choose the logistic regression ML model.
- Use the most prioritized feature with the target class to create a classification model and assess its accuracy.
- Add the second-highest prioritized feature to the previous step and evaluate the model.
- Repeat the same process with the next feature until the last feature.
- Identify the optimal number of features for high sensitivity and specificity.

These features that provide optimal results are the ones selected through the one-way analysis of variance test.

d: PRINCIPAL COMPONENT ANALYSIS (PCA)

Principal Components Analysis (PCA) is a well-known statistical approach widely used for dimensionality reduction while retaining the most informative data. PCA helps to identify significant patterns or features from large datasets by transforming them into lower-dimensional representations.

F. PERSON IDENTIFICATION USING MULTIPLE ML CLASSIFIERS

In this study, the user authentication procedure has been examined with 14 machine learning and seven deep learning classification methods. Fig. 3 illustrates a generalized version of the ML and DL models employed in the study.

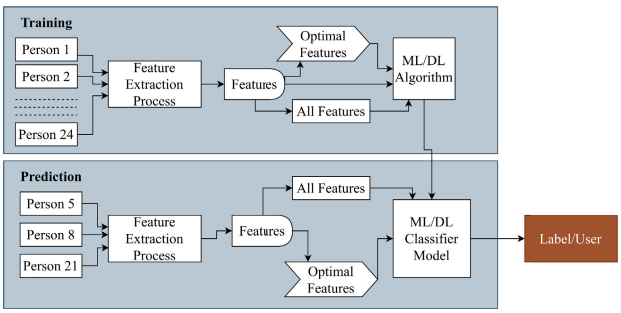

FIGURE 3. Process Flow for Using Machine and Deep Learning Models in the System.

The classification algorithms under the machine learning discipline implemented in this study are briefly illustrated in the following section.

1) SUPPORT VECTOR MACHINE (SVM)

A Support Vector Machine (SVM) decision algorithm is a specifically optimized "hyperplane" that distinguishes between observations that belong to one class and those that do not. The ability of the ideal hyperplane to maximize the boundary between classes distinguishes it [57], [58]. Fig. 4 shows how SVM methodology works by the hyperplane concept.

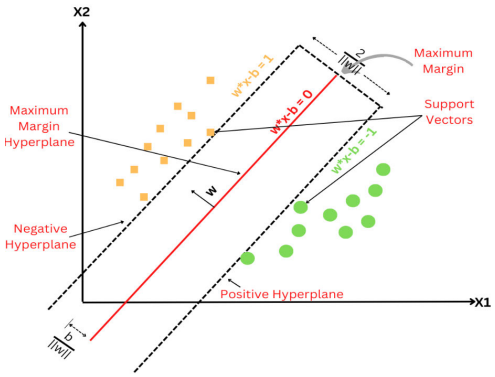

FIGURE 4. SVM working mechanism with attributes.

2) DECISION TREE (DT)

The Decision Tree Approach divides a population into "branches" with a root node in the center and "child" nodes at the branches' tips. Each branch represents a test, each leaf node symbolizes a class, and the path from the root to the leaf represents a decision-making process [59]. Fig. 5 depicts an example of the decision tree.

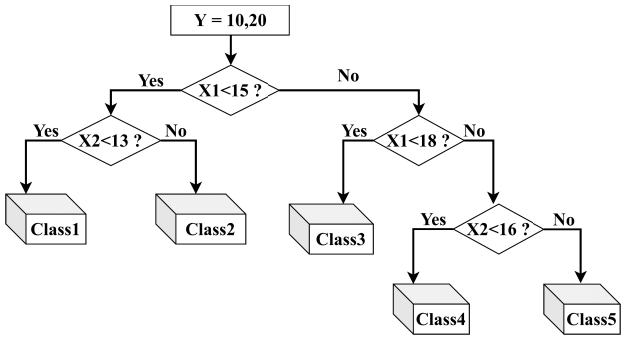

FIGURE 5. Binary target variable-based example of a decision tree.

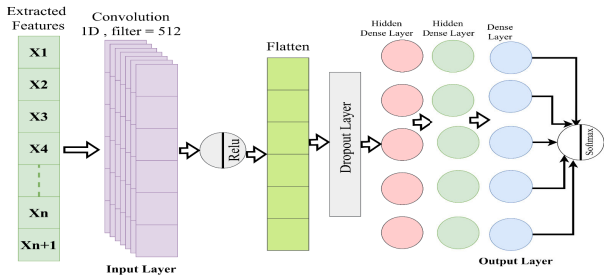

FIGURE 6. Convolutional Neural Network 1D.

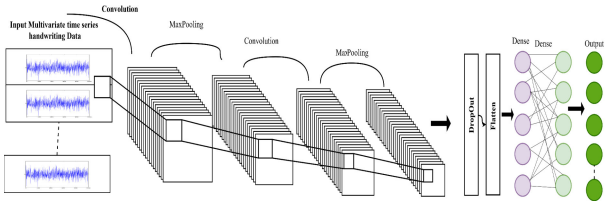

FIGURE 7. Convolutional Neural Network 2D.

3) BOOSTING ALGORITHM

The boosting approach encompasses three major concepts: Bagging, Boosting, and Stacking. In gradient boosting, a phase additive model is used to minimise the differential loss function by using a series of decision trees as weak learners and a gradient descent optimisation process [60].

4) LOGISTIC REGRESSION (LR)

For forecasting categorical outcomes and discriminant analysis, the logistic regression (LR) model is widely used [61]. The LR is represented using Equation (12) as follows:

$$\text{Predicted}, y = \frac{e^{(B_0+B_1X)}}{1+e^{(B_0+B_1X)}} \tag{12}$$

5) RANDOM FOREST (RF)

Random Forest (RF) makes predictions by averaging the outcomes of numerous decision trees in regression problems or calculating the majority vote in classification problems [62]. The RF model's calculation was obtained using Equation (13)

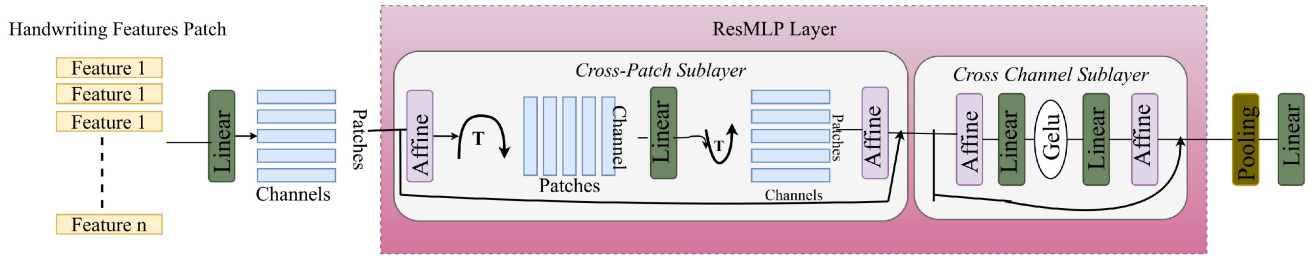

FIGURE 8. Model Architecture of Residual Multi-Layer Perceptrons.

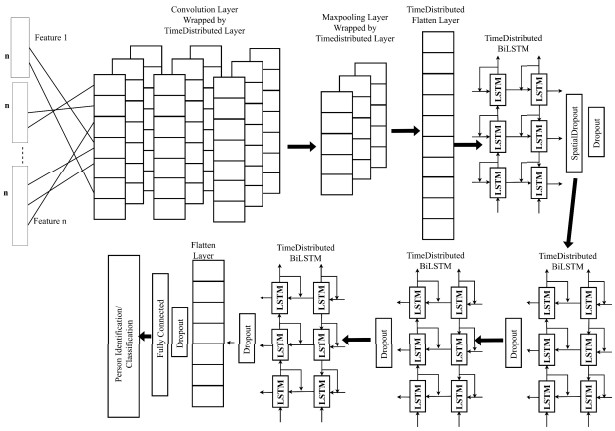

FIGURE 9. CNN-BiLSTM Model Architecture.

as follows:

$$\text{Entropy} = -mlog_2(m) - nlog_2(n) \tag{13}$$

6) K-NEAREST NEIGHBOR (KNN)

K Nearest Neighbors (KNN) algorithm is based on the idea of proximity, where each new data point is classified by analyzing its k closest neighbours and assigning it to the class that is most frequently represented among them [63].

7) NAÏVE BAYES (NB)

Naive Bayes calculates the likelihood of each class and selects the class with the highest likelihood as the best option for the prediction [64]. Naïve Bayes Theorem is calculated according to the Equation (14):

$$P(m|n) = \frac{P(n|m) \times P(m)}{P(n)} \tag{14}$$

where $P(m\|n)$ is the posterior probability, $P(m)$ and $P(n)$ are the class prior and predictor prior probability, and $P(nm)$ is the likelihood.

8) STOCHASTIC GRADIENT DESCENT (SGD)

Stochastic Gradient Descent (SGD), an optimization algorithm involves computing the gradient of a loss function concerning the model's weights and biases and updating them accordingly [65].

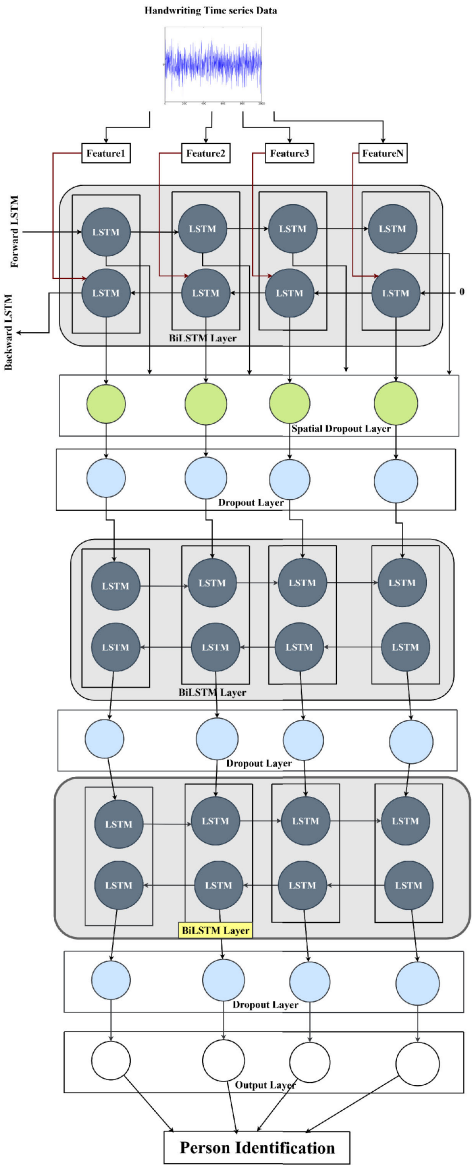

FIGURE 10. BiLSTM Model Architecture.

G. USER AUTHENTICATION USING DEEP LEARNING APPROACH

The DL algorithms use numerous layers to extract meaningful information from raw data, and their hierarchical structure enables them to represent complex functions with

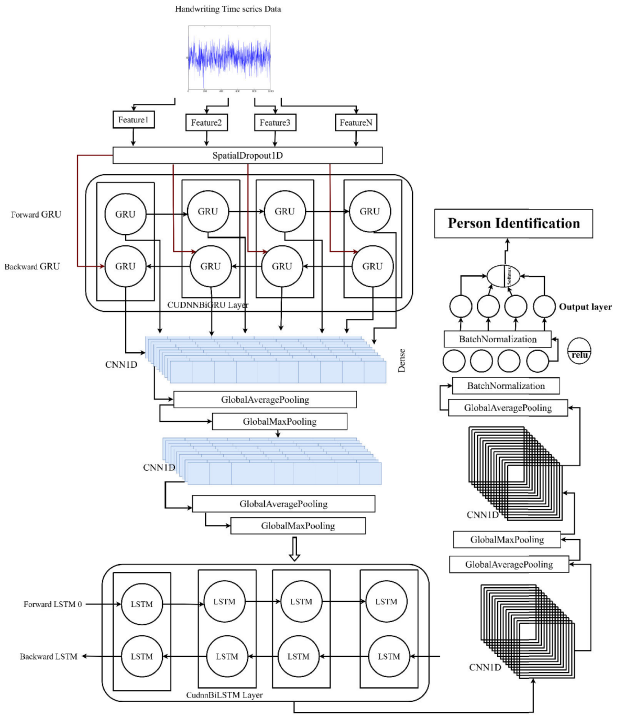

FIGURE 11. Fusion of Time-Distributed BiGRU, BiLSTM, and Convolution Neural Network (Hybrid Architecture).

Layer (type)	Output Shape	Parameter
Spatial Dropout Layer (Spatia1Dropout1D)	(None, 91, 91)	0
Bidirectional Layer (LSTM)	(None, 91, 32)	10464
Convolution Layer (Conv1D)	(None, 91, 16)	528
Global Average Pooling	(None, 16)	0
Reshape Layer	(None, 1, 16)	0
Global Max Pooling	(None, 16)	0
Reshape Layer	(None, 1, 1, 16)	0
Convolution Layer (Conv1D)	(None, 1, 1, 32)	544
Reshape Layer	(None, 1, 32)	0
Global Average Pooling	(None, 32)	0
Reshape Layer	(None, 1, 32)	0
Global Max Pooling	(None, 32)	0
Reshape Layer	(None, 1, 32)	0
Bidirectional Layer (LSTM)	(None, 1, 128)	50176
Convolution Layer (Conv1D)	(None, 1, 512)	66048
Reshape Layer	(None, 16, 32)	0
Global Average Pooling	(None, 32)	0
Reshape Layer	(None, 1, 32)	0
Global Max Pooling	(None, 32)	0
Reshape Layer	(None, 1, 32)	0
Convolution Layer (Conv1D)	(None, 1, 512)	16896
Global Average Pooling	(None, 512)	0
BatchNormalization Layer	(None, 512)	2048
Dense Layer	(None, 48)	24624
BatchNormalization Layer	(None, 48)	192
Dense Layer	(None, 24)	1176
Activation Function	(None, 24)	0
Total params	172,696	
Trainable params	171,576	
Non-trainable params	1,120	

FIGURE 12. Summary of the Hybrid Architecture Model.

fewer parameters [66]. As the field of computer vision has progressed recently, some researchers have proposed transforming time-series data into images and utilizing Convolutional Neural Networks (CNNs) as the classifier.

TABLE 6. Performance evaluation metrics description.

Performance Evaluation Metrics	Equation
Accuracy Score (%)	$\frac{TP+TN}{TP+TN+FP+FN} \times 100\%$
Precision	$\frac{TP}{TP+FP}$
Recall	$\frac{TP}{TP+FN}$
Specificity	$\frac{TN}{TN+FP}$
F1-Score	$2 \times \frac{Recall \times Precision}{Precision+Recall}$
Support	Frequency of each class
Execution Time (seconds)	Finish Time-Start Time
Area Under Curve (AUC)	-

TABLE 7. Data characteristics of both databases 1 and 2.

Person	No. of Words	Iterations	Each Person No. of Samples	Training Split	Testing Split
Person 1	10	5	50	40	10
Person 2	10	5	50	40	10
...	...	...	...	....	10
Person24	10	5	50	40	10
		Dataset 1	1200	960	240
		Dataset 2	1200	960	240
		Total	2400	1920	480

TABLE 8. Accuracy Vs Number of Features in ANOVA-F test.

Numbers of Selected Feature	Mean Score	Best Score	Std Score
1	0.204098	0.221311	0.00931
2	0.201366	0.221311	0.012283
3	0.281421	0.344262	0.024802
...	...	...	...
...	...	...	...
7	0.363934	0.409836	0.029599
8	0.365574	0.434426	0.029142
9	0.369672	0.42623	0.029806
10	0.374044	0.467213	0.030995
...	...	...	...
...	...	...	...
86	0.923224	0.967213	0.022145
Highest Accuracy = 87	0.92623	0.989016	0.022297
...	...	...	...
...	...	...	...
91	0.924863	0.967213	0.022003

This approach has the potential to identify individuals and differentiate between healthy and patient by acquiring knowledge of extracted features from the raw input data [63]. In this research, various Deep Neural Network models, such as Artificial Neural Networks (ANN), Convolutional Neural Networks (CNN), Residual Multilayer Perceptron (ResMLP), Bidirectional Long Short-Term Memory (BiLSTM), CNN-BiLSTM, and a Hybrid model (incorporating features of CNN, CuDNNBiGru, and CuDNNBiLSTM) have been evaluated on the training and testing datasets to classify handwriting time-series data.

TABLE 9. The optimal number of features selected by the ANOVA F test.

Best Mean Accuracy	Optimal Number of Features that obtained the best accuracy	Test Accuracy
92.6%	87%	98.0%

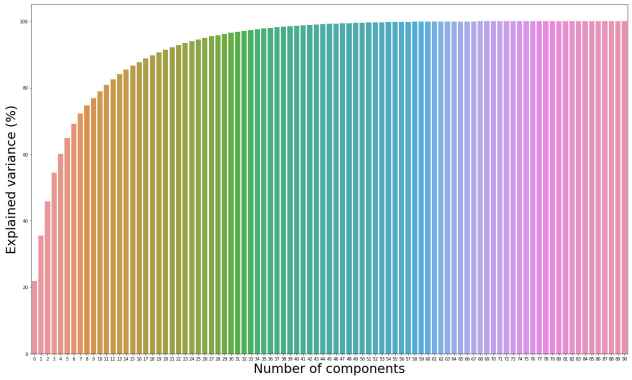

FIGURE 13. Optimal number of components that give the best accuracy.

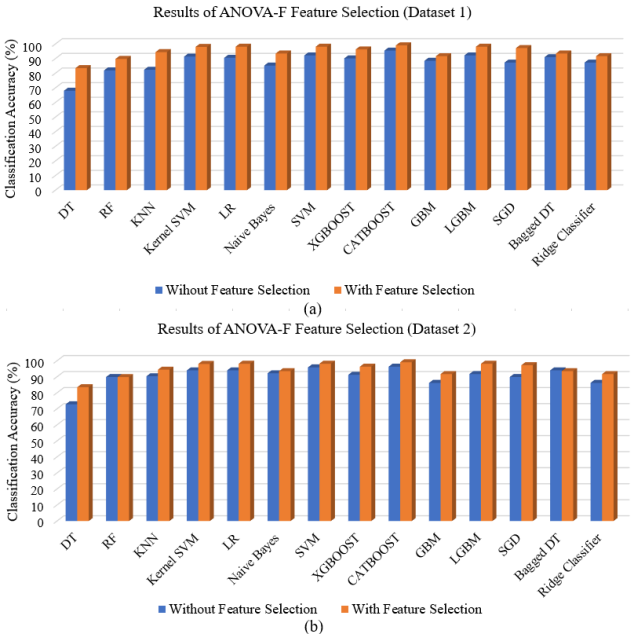

FIGURE 14. Visualization of the comparison of the results without and with ANOVA-F Feature Selection: (a) Dataset 1, (b) Dataset 2.

Deep Learning Architecture The proposed deep learning architectures comprised various layers and auxiliary components, including input layers, dense layers, pooling layers, reshape layers, batch normalization layers, dropout layers, flatten layers and activation functions, loss functions, and optimizers. The key layers responsible for the classification task in the various models comprised bidirectional LSTM layers, Convolution1D layers, Conv2D layers, Time distributed wrapped layers, bidirectional CuDNNGRU layers, and bidirectional CuDNNLSTM layers. This study has also

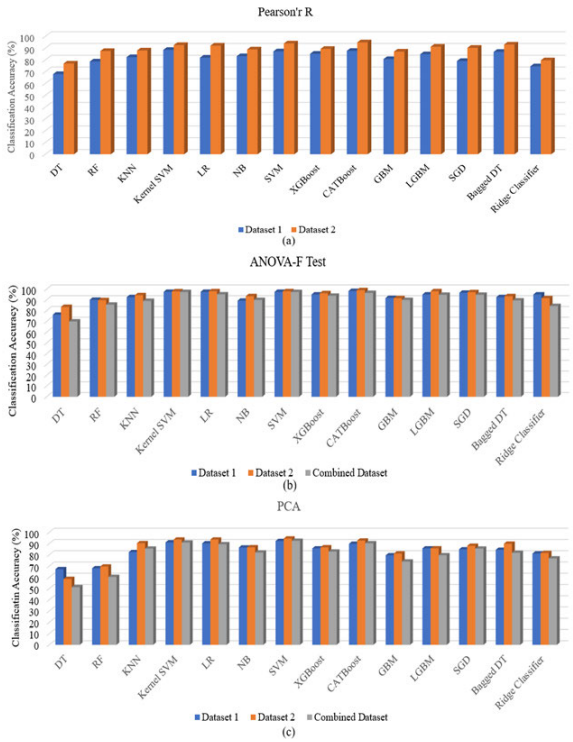

FIGURE 15. Test-set Accuracy of Dataset 1, Dataset 2 and their combined one with different feature selection approaches, (a) Pearson's R, (b) ANOVA-F Test, and (c) PCA.

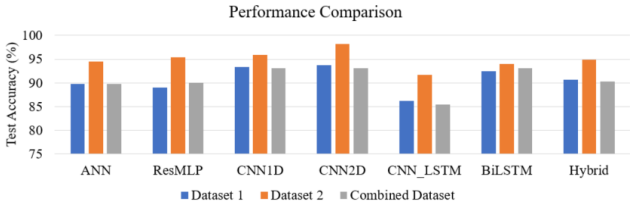

FIGURE 16. Performance comparison with three different versions of the database.

introduced a novel hybrid DL architecture. The architectures evaluated in this paper are depicted in the following illustrations.

1) CONVOLUTIONAL NEURAL NETWORKS WITH 1D AND 2D

Fig. 6 illustrates the CNN−1D model architecture used in this study. It has a single convolution layer that uses a rectified linear unit (ReLU) activation function and 1×1 kernels with a stride of 1 pixel. After the convolution layers, the final classification is performed using fully-connected layers. The architecture of the 2D CNN model utilized in this paper is illustrated in Fig. 7. It includes two convolution layers, each using 128 and 64 filters with two strides, respectively. The pooling process employs MaxPooling. Following the pooling process, the outputs are combined and flattened before being sent to a fully connected layer for prediction.

TABLE 10. Performance Evaluation of different ML classifiers on dataset 1, dataset 2, and their combined ones without feature selection.

Model	Test Accuracy (%)			Precision			Recall			F1-Score			Support			Specificity			Execution Time (in Seconds) Model Train		
	Dataset 1	Dataset 2	Combined	Dataset 1	Dataset 2	Combined	Dataset 1	Dataset 2	Combined	Dataset 1	Dataset 2	Combined	Dataset 1	Dataset 2	Combined	Dataset 1	Dataset 2	Combined	Dataset 1	Dataset 2	Combined
Decision Tree	68.03	72.82	67.45	0.73	0.77	0.72	0.68	0.73	0.67	0.68	0.72	0.68	244	217	461	0.98	0.98	0.99	0.32	0.20	1.07
RF	81.96	89.87	83.74	0.84	0.91	0.85	0.82	0.90	0.84	0.82	0.89	0.83	244	217	461	0.99	0.99	0.99	0.15	0.22	0.75
K-NN	82.37	90.32	85.69	0.84	0.91	0.88	0.82	0.90	0.86	0.82	0.90	0.86	244	217	461	0.99	0.99	0.99	0.003	0.02	0.001
Kernel SVM	91.39	94.00	90.68	0.94	0.95	0.92	0.91	0.94	0.91	0.92	0.94	0.91	244	217	461	0.99	0.99	0.99	0.08	0.11	0.50
LR	90.57	94.00	91.55	0.92	0.95	0.92	0.91	0.94	0.92	0.91	0.94	0.91	244	217	461	0.99	0.99	0.99	1.36	0.55	4.12
Naïve Bayes	85.24	92.17	86.34	0.86	0.93	0.88	0.85	0.92	0.86	0.85	0.92	0.86	244	217	461	0.99	0.99	0.99	0.005	0.005	0.01
SVM	92.21	95.86	93.28	0.92	0.96	0.94	0.92	0.96	0.93	0.92	0.96	0.93	244	217	461	0.99	0.99	0.99	0.07	0.04	0.25
XGBoost	90.16	91.25	89.81	0.92	0.93	0.92	0.90	0.91	0.90	0.90	0.91	0.90	244	217	461	0.99	0.99	0.99	40.1	2.73	22.0
CatBoost	95.49	96.32	93.93	0.96	0.97	0.95	0.95	0.96	0.94	0.95	0.96	0.94	244	217	461	0.99	0.99	0.99	425.5	405.8	867.3
GBM	88.52	86.18	83.73	0.89	0.90	0.86	0.88	0.87	0.84	0.88	0.87	0.84	244	217	461	0.86	0.99	0.99	91.4	82.0	272.4
Light GBM	92.21	91.71	89.80	0.93	0.93	0.91	0.92	0.92	0.90	0.92	0.92	0.90	244	217	461	0.99	0.99	0.99	11.42	12.1	27.90
Bagged DT	87.30	89.87	87.41	0.93	0.95	0.92	0.92	0.95	0.91	0.92	0.95	0.91	244	217	461	0.99	0.99	0.99	4.69	2.50	9.57
SGD	90.99	94.00	90.67	0.86	0.92	0.89	0.84	0.91	0.88	0.84	0.91	0.88	244	217	461	0.99	0.99	0.99	0.14	0.109	0.73
Ridge Classifier	87.30	86.18	82.21	0.89	0.85	0.85	0.87	0.86	0.82	0.88	0.85	0.81	244	217	461	0.87	0.99	0.99	0.03	0.03	0.03

2) RESIDUAL MULTI-LAYER PERCEPTRONS(RESMLP)

We also implemented the ResMLP model on our dataset to compare and understand the system's efficiency. Fig. 8 shows the ResMLP architecture [67] that has been implemented on the handwriting database.

3) BIDIRECTIONAL LSTM

Long-short-term memory Networks (LSTMs) are a type of neural network well-suited for learning from sequential input and can effectively handle time series data of varying lengths [68]. Due to their exceptional memory retention abilities, LSTMs have also effectively processed handwritten time series signals. Fig. 10 demonstrates the BiLSTM architecture implementation. Four BiLSTM Layer with Dropout Layer is interconnected with a fully connected layer for classification.

4) CNN-BILSTM

To achieve efficient performance, we have applied the CNN-BiLSTM architecture to the extracted time series features. In this framework, CNN layers are used to extract features from the input data, whereas BiLSTMs are used for sequence prediction. As compared to other methods that convert the time series into images, our model makes full use of the original raw data. Layers of the CNN are built using kernels that iteratively process the sequence in two dimensions. A visual representation of the CNN-BLSTM model for multivariate time data is presented in Fig. 9.

5) HYBRID ARCHITECTURE

A novel hybrid architecture is proposed in this research for the classification of handwriting data. The architecture combines a CNN, Bidirectional CuDNNGRU model with a Bidirectional CuDNNLSTM model. The emphasis of our research is on time series data prediction, an area where GRU and LSTM models may be extremely useful. Fig. 11 shows the combination of the time-distributed BiGRU, BiLSTM, and CNN. The process begins by inputting the features into the BiGRU layer. Subsequently, the output from the BiGRU layer is used as input for the CNN1D layer. The resulting output from the CNN1D layer then feeds into a dynamic BiLSTM layer. The outcomes obtained from the BiLSTM layer are employed in constructing a fully connected layer, which performs the classification task. Fig. 12 illustrates the various levels and parameters used in this architecture.

H. PERFORMANCE EVALUATION METRICS

In this paper, the proposed system for user identification is evaluated using several performance evaluation metrics such as the accuracy score, recall/sensitivity, precision, F1-score, support, and area under the curve (AUC) to assess its performance. A confusion matrix was constructed to quantify the ratio of correct to incorrect predictions across 48 classes. The definitions of true positive (TP), false positive (FP), true negative (TN), and false negative (FN) were used in the computation of accuracy, recall, precision, confusion matrix, and f1-scores. The mathematics behind performance evaluation metrics are shown in Table 6.

IV. EXPERIMENTAL RESULTS AND DISCUSSION

A. EXPERIMENTAL SETUP

This study conducted experiments using two databases, each of which contained data regarding 24 individuals. The whole database and the segmentation criteria used in this investigation are summarized in Table 7. The dataset used for classifying the users was split into training and testing sets, each containing 80% and 20% of the total dataset, respectively.

B. FEATURES OBTAINED BY SELECTION APPROACHES

1) PEARSON'S R CORRELATION COEFFICIENT

Since in this study, two datasets are used, each consisting target value of 24 classes, we determined the correlation between each feature and the target class using Pearson's correlation coefficient for both datasets and took threshold significant value as r_{xy}>0.04 for Dataset 1 and r_{xy}>0.09 for Dataset 2, Out of 91 features 45 (Dataset 1) and 47 (Dataset 2) features passed these significant threshold values.

2) ANOVA

ANOVA test is used to assess a total of 91 retrieved features. Table 8 illustrates the feature selection procedure used in the ANOVA-F test on Dataset 1. Eighty-seven (87) out of the 91 features were judged superior and retrieved for consideration after moving on with the ANOVA test, which is shown in Table 9. The reason for keeping so many characteristics is that all 87 of them have been determined to be essential to raising the system's accuracy.

3) MUTUAL INFORMATION

Based on the results, the average accuracy is 92.5%, whereas the optimal number of features obtained with the best accuracy is 91%, and the test accuracy is 98%. In the MI approach, the system achieves the best accuracy when using all 91 features in combination with the LR classifier.

4) PRINCIPAL COMPONENT ANALYSIS

Applying PCA to Dataset 1 revealed that 44 principal components out of the original 91 features were sufficient to achieve optimal accuracy, as shown in Fig. 13.

C. RESULTS AND DISCUSSION BY ML-BASED APPROACH

In this experiment, 14 ML techniques (SVM, DT, RF, KNN, Kernel-SVM, LR, CATBOOST, XGBOOST, SGD, Bagged DT, GBM, LIGHTGBM, Ridge Classifier, Naïve Bayes) have been implemented on Dataset 1 and Dataset 2, as well as the combined Dataset. Experiments were conducted primarily in two divisions, namely, without and with feature selection. Multiple experiments in various angles have been carried out to analyze the handwriting datasets.

TABLE 11. Performance Evaluation of Dataset 1, Dataset 2 and Combined Dataset after K-Fold cross-validation.

	Dataset 1= 10 Fold		Dataset 2=10 Fold		Combined Dataset=6 Fold	
Model	**Best Accuracy**	**Standard Deviation**	**Best Accuracy**	**Standard Deviation**	**Best Accuracy**	**Standard Deviation**
DT	77.87%	4.45%	82.41%	2.88%	70.43%	2.65%
RF	91.80%	3.74%	89.81%	2.47%	84.78%	1.82%
KNN	93.44%	2.35%	93.52%	1.49%	89.57%	1.36%
Kernel SVM	98.36%	1.76%	98.15%	1.83%	96.09%	1.28%
LR	94.26%	1.36%	98.15%	2.49%	94.35%	2.15%
Naive Bayes	87.70%	1.92%	93.52%	1.58%	89.57%	1.86%
SVM	98.36%	1.76%	98.15%	1.83%	95.65%	1.18%
XGBOOST	95.08%	2.24%	97.22%	3.21%	92.17%	1.06%
CATBOOST	96.72%	1.74%	98.15%	1.84%	96.09%	1.31%
GBM	92.62%	2.42%	93.52%	2.39%	90.43%	2.04%
LGBM	95.90%	2.01%	97.22%	1.81%	93.48%	1.55%
SGD	95.90%	2.25%	97.22%	1.87%	94.35%	1.99%
Bagged DT	93.44%	1.96%	95.37%	2.89%	88.70%	2.29%
Ridge Classifier	95.90%	2.46%	91.67%	2.88%	85.65%	1.98%

TABLE 12. Individual Task Accuracy of Dataset 1 using 10 fold cross validation.

	Words(Task)									
Model	**Task 1(%)**	**Task 2(%)**	**Task 3(%)**	**Task 4(%)**	**Task 5(%)**	**Task 6(%)**	**Task 7(%)**	**Task 8(%)**	**Task 9(%)**	**Task 10(%)**
DT	72.0	87.57	59.72	65.72	62.78	68.12	72.58	79.78	71.31	65.63
RF	86.0	92.78	68.82	75.95	75.34	76.48	74.48	82.95	81.54	89.01
K-NN	90.7	91.62	82.01	81.95	89.01	87.54	88.01	90.84	79.92	89.86
K-SVM	91.0	94.26	89.54	79.12	87.05	79.21	91.47	89.22	91.98	91.56
LR	98.0	95.90	91.47	89.84	93.11	93.56	91.87	96.74	94.31	97.37
Naïve B.	89.0	86.89	73.68	76.32	65.79	73.68	68.42	68.42	76.32	65.79
SVM	91.0	96.72	86.84	86.84	92.11	92.11	92.11	94.74	94.74	92.11
XGBOOST	90.7	93.44	71.05	73.68	71.79	81.58	81.58	78.95	73.68	76.32
CATBOOST	98.00	96.72	89.99	90.47	94.87	97.01	95.46	94.74	100.0	97.37
GBM	73.0	91.80	50.00	50.00	54.74	65.26	57.37	62.63	74.10	65.26
LGBM	100.0	92.62	84.21	84.21	89.62	91.47	89.21	94.11	86.84	84.21
Bagged DT	88.0	95.08	84.21	86.84	84.62	86.84	92.11	97.37	97.44	90.47
SGD	98.0	92.62	90.47	77.68	79.32	84.95	82.95	84.58	89.05	89.21
Ridge Classifier	95.0	92.62	89.47	73.68	76.32	78.95	78.95	81.58	82.05	84.21

TABLE 13. Individual task accuracy of combined dataset using 6 fold cross validation.

	Words(Task)									
Model	**Task 1(%)**	**Task 2(%)**	**Task 3(%)**	**Task 4(%)**	**Task 5(%)**	**Task 6(%)**	**Task 7(%)**	**Task 8(%)**	**Task 9(%)**	**Task 10(%)**
DT	60.0	79.51	48.72	52.63	57.89	55.26	57.89	65.79	56.41	52.63
FR	80.0	90.98	65.79	71.05	71.79	73.68	73.68	78.95	73.68	84.21
K-NN	85.7	88.52	76.32	78.95	84.21	81.58	84.21	86.84	76.92	84.21
K-SVM	85.0	94.26	84.21	78.95	82.05	75.71	89.47	86.84	89.47	89.47
LR	95.0	95.90	89.47	86.84	92.11	92.11	89.47	94.74	92.31	97.37
Naïve B.	85.0	86.89	73.68	76.32	65.79	73.68	68.42	68.42	76.32	65.79
SVM	85.0	96.72	86.84	86.84	92.11	92.11	92.11	94.74	94.74	92.11
XGBOOST	85.7	93.44	71.05	73.68	71.79	81.58	81.58	78.95	73.68	76.32
CATBOOST	95.0	96.72	89.47	89.47	94.87	97.37	94.74	94.74	100.0	97.37
GBM	65.0	91.80	50.00	50.00	44.74	55.26	47.37	52.63	64.10	55.26
LGBM	100.0	92.62	84.21	84.21	84.62	89.47	84.21	92.11	86.84	84.21
Bagged DT	80.0	95.08	84.21	86.84	84.62	86.84	92.11	97.37	97.44	89.47
SGD	95.0	92.62	89.47	73.68	76.32	78.95	78.95	81.58	82.05	84.21
Ridge	90.0	92.62	81.58	86.84	82.05	86.84	84.21	92.11	89.47	92.11

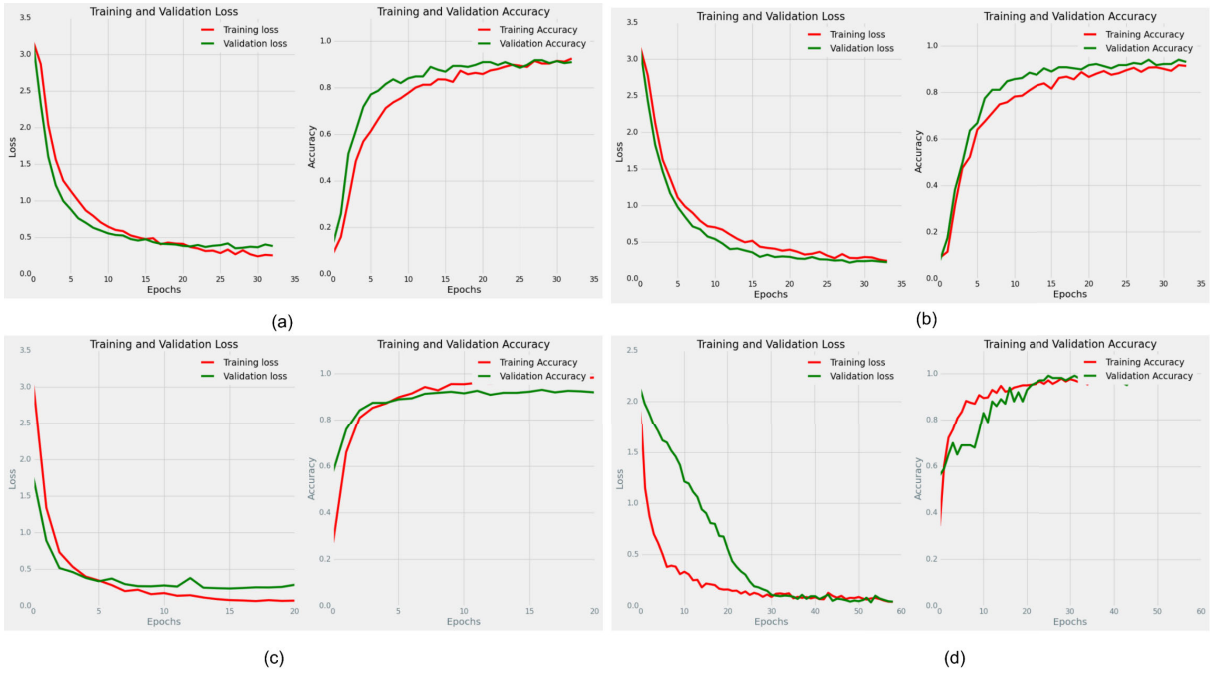

FIGURE 17. AUC Plot of Training and Validation Loss and Accuracy for (a) BiLSTM Model applied on Dataset 1 (b) BiLSTM Model applied on Dataset 2 (c) CNN1D Model applied on the combined dataset(48 persons) (d) Hybrid Model applied on the dataset making up by 10 persons sample from both.

TABLE 14. Test-set accuracy of dataset 1 and dataset 2 by implementing PEARSON'S r correlation methodology.

Model	Dataset 1, threshold > 0.04, 45 features	Dataset 2, threshold > 0.04, 47 features
Decision Tree	68.03%	76.96%
Random Forest	78.69%	87.56%
KNN	82.38%	88.02%
Kernel SVM	88.52%	92.63%
Logistic Regression	81.97%	92.17%
Naive Bayes	83.20%	88.94%
SVM	87.30%	94.01%
XGBOOST	85.25%	89.40%
CATBOOST	87.70%	94.93%
GRADIENTBOOST	80.74%	87.10%
Light GBM	84.84%	91.24%
SGD	79.10%	90.32%
Bagged Decision Tree	86.89%	93.09%
Ridge Classifier	74.59%	79.72%

TABLE 15. Performance evaluation of different ML classifiers using Dataset 1, Dataset 2, and Combined Dataset after PCA transformation.

Model	Dataset 1	Dataset 2	Combined Dataset
Decision Tree	67.21%	58.53%	51.19%
Random Forest	68.03%	69.59%	60.30%
KNN	82.38%	90.32%	85.47%
Kernel SVM	90.98%	93.55%	90.89%
Logistic Regression	90.16%	93.55%	89.37%
Naive Bayes	86.48%	86.64%	82.00%
SVM	92.21%	94.47%	92.41%
XGBOOST	85.66%	86.64%	82.86%
CATBOOST	89.75%	92.63%	90.24%
GBM	79.51%	81.11%	73.97%
LGBM	85.66%	85.71%	79.61%
SGD	84.84%	88.02%	85.47%
Bagged Decision Tree	84.43%	89.86%	81.78%
Ridge Classifier	81.15%	81.57%	76.79%
Principal Components	PC = 44	PC = 45	PC=46

1) WITHOUT FEATURE SELECTION

Table 10 shows the performance results of various ML models on two datasets (Dataset 1 and Dataset 2) and their combination (Combined Dataset). The models were evaluated using evaluation metrics: Test Accuracy, Precision, Recall, F1-Score, and Support.

For the individual datasets, the best-performing models were Kernel SVM and Logistic Regression (91.39% and 90.57%, respectively, on Dataset 1 and 94.00% on Dataset 2) and CATBOOST (93.93%) for the combined dataset. Overall, the results suggest that SVM and Logistic Regression are the best models for this particular problem.

K-Fold Cross Validation

Table 11 compares different models applied to two datasets and their combined datasets.

Individual Task/Word Evaluation using K-Fold Table 12 shows the Individual Task Accuracy of Dataset 2 using 6-fold cross-validation and concluded that the Logistic Regression (LR) model has the highest score. Table 13 shows the Individual Task Accuracy of the combined Dataset using 6-fold cross-validation.

TABLE 16. Test set accuracy of different ML classifiers using 87 Selected Features by ANOVA F test (10 fold + Hyper parameter tuned).

	Dataset 1		Dataset 2		Combined Dataset	
Model	Best Accuracy	Standard Deviation	Best Accuracy	Standard Deviation	Best Accuracy	Standard Deviation
DT	76.23%	3.26%	83.49%	3.15%	70.00%	1.91%
RF	90.16%	3.40%	89.81%	2.56%	85.65%	2.59%
K-NN	92.62%	1.93%	94.44%	1.98%	89.13%	0.89%
K-SVM	97.54%	1.68%	98.02%	1.94%	97.39%	1.49%
LR	97.54%	1.83%	98.15%	2.85%	95.22%	2.63%
Naïve B.	89.34%	2.56%	93.52%	1.49%	90.00%	1.93%
SVM	97.54%	1.68%	98.15%	1.96%	97.39%	1.48%
XGBOOST	95.08%	2.30%	96.30%	3.16%	93.91%	2.12%
CATBOOST	98.36%	1.99%	99.07%	2.67%	96.52%	1.34%
GBM	91.80%	2.32%	91.67%	1.67%	90.00%	2.38%
LGBM	95.08%	1.55%	98.13%	2.55%	94.78%	1.53%
Bagged DT	96.72%	2.32%	97.22%	2.11%	94.78%	2.32%
SGD	92.62%	2.10%	93.52%	2.92%	89.57%	2.45%
Ridge Classifier	95.08%	2.01%	91.67%	3.38%	84.35%	1.72%

2) WITH FEATURE SELECTION

We extracted the important features using different feature selection techniques to conduct the test evaluation.

a: PEARSON'S R CORRELATION

The dataset 1 had 45 features with a threshold larger than 0.04, however, the dataset 2 contained 47 features with the same threshold. Table 14 represents the results of the accuracy of each algorithm's performance. The findings of this research reveal that SVM algorithms, CATBOOST, and the light GBM performed well on both datasets.

b: ANOVA F TEST (10 FOLD + HYPER-PARAMETER TUNED)

Table 16 presents the test set accuracy of several ML classifiers using 87 chosen features as determined by the ANOVA F test (10-fold cross-validation and hyperparameter tuning). The findings indicate that the kernel SVM, logistic regression, SVM, and CATBOOST models are superior to the other models for the classification job. Additional investigation and refinement of these models may result in greater accuracy.

c: WITH PCA SELECTED FEATURES

The results presented in Table 15 present the performance evaluation of various ML classifiers using Dataset 1, Dataset 2, and the combined dataset after applying PCA transformation. The number of Principal Components (PCs) used in the analysis was 44, 45, and 46. The best accuracy was achieved by the CATBOOST classifier, with 92.63% on Dataset 2, followed by the SVM classifier, with 94.47% on Dataset 2. Fig. 14 depicts the classification accuracy of dataset 1, dataset 2, and the combined dataset with the selected features. Fig. 15 selection using Dataset 1 and Dataset 2.

TABLE 17. A Comparison of model performance on datasets with and without feature selection for dataset 2.

Model	Without Feature Selection Test Acc.	Anova-F tested Features (87)	PCA dimension reduced features (45)
ANN	94.47%	95.93%	96.85%
ResMLP	95.39%	96.85%	95.00%
CNN1D	95.85%	96.85%	96.85%
CNN2D	98.15%	97.85%	97.39%
CNN_LSTM	91.70%	96.93%	93.32%
BiLSTM	94.00%	96.47%	98.31%
Hybrid	94.93%	96.47%	96.93%

D. RESULTS AND DISCUSSION BY DL-BASED APPROACH

This study employed 7 deep learning-based models (ANN, ResMLP, CNN1D, CNN2D, CNN-BiLSTM, and Novel Hybrid Model) to prove the practicality, robustness, and efficiency of our experiment. In the experimental phase, we conducted two classification scenarios: classification with and without selected features. Experiments were conducted using various angles and approaches such as with varying numbers of person classifications, including 5, 10, 15, 20, 24, and 48 persons.

1) WITHOUT FEATURE SELECTION

The classification efficiency of 7 deep learning models is highlighted in Table 18. These tables demonstrate the assessment of the models utilizing diverse performance evaluation metrics on Dataset 1, Dataset 2, and the combined Dataset without Feature Selection.

a) Performance Comparison with Two Datasets and Combined Dataset We have evaluated two datasets and their combined counterparts. As depicted in Fig. 16, the results demonstrate that among the three datasets, Dataset 2

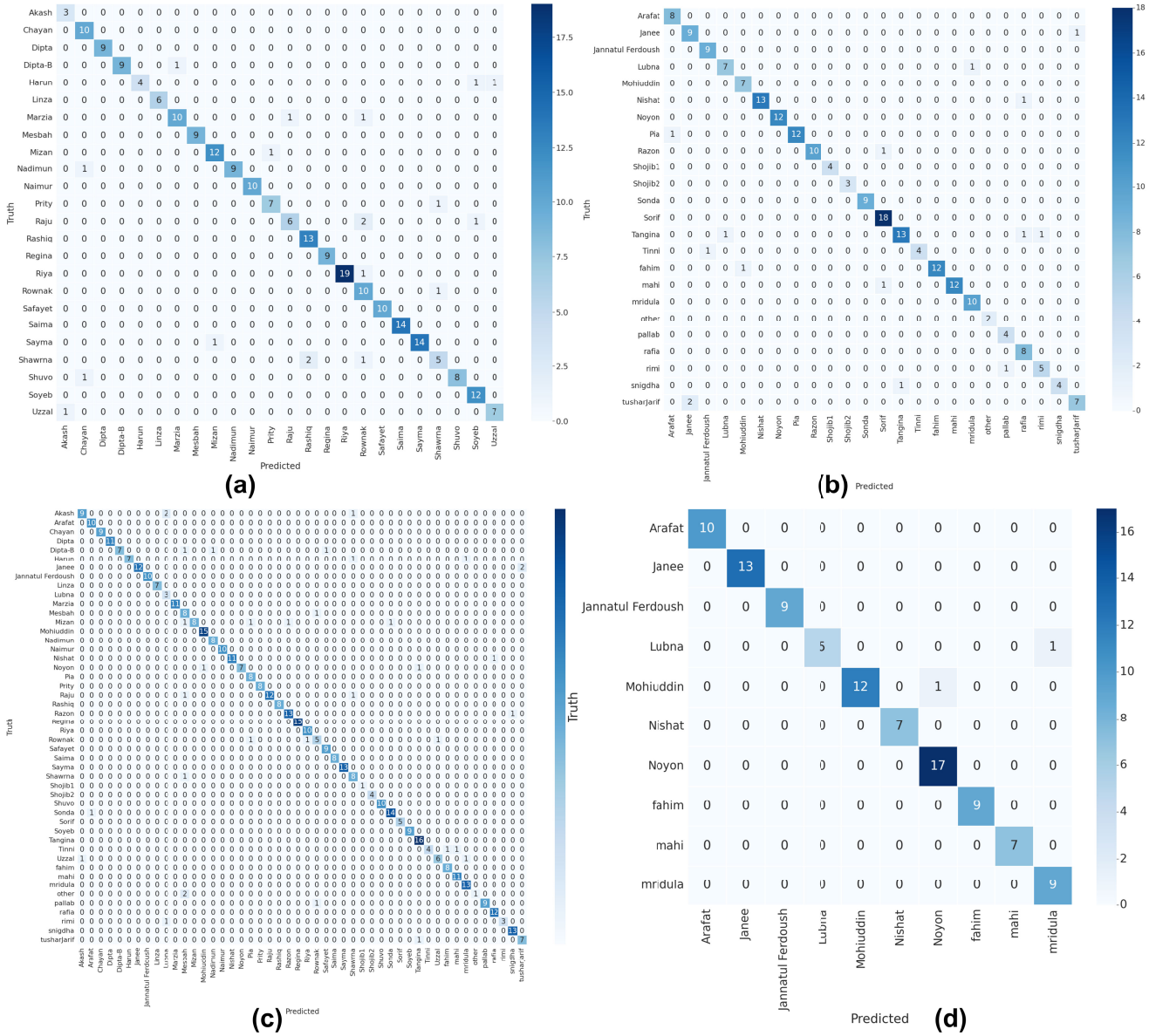

FIGURE 18. A Confusion Matrix (a) 24 Classes from Dataset 1 using Bidirectional LSTM Model (b) 24 Classes from Dataset 2 using the Hybrid Model (c) 48 Classes from combined Model using the CNN2D Model (d) Hybrid Model implementation taking 10 Persons from database.

yields the optimal performance. Fig. 17 presents the learning curves (AUC plot) of the different models applied on Dataset 1, Dataset 2, and their combined ones, demonstrating the fluctuation in loss and accuracy in each epoch during both the training and testing phases. The confusion matrix, depicted in Fig. 18, provides a visual representation of the performance of the models implemented on Dataset 1, and Dataset 2, and combined Dataset with a contingency table.

b) Evaluation Based on Different Numbers of Persons

Table 18 also shows the comparison of the results of tests conducted on datasets that differed in 5, 10, 15, 20, 24, and 48 persons. The findings revealed that the system's performance dropped ever-so-slightly with increasing numbers of users, but by no means significant.

2) WITH FEATURE SELECTION

A total of 87 optimal features were by ANOVA-F test, whereas 45 features by PCA out of 91 extracted features were utilized on Dataset 2 to evaluate the effect of feature selection on the model's overall performance, and was compared to that of the features without a selection mechanism. The results presented in Table 17 reveal the effect of the feature selection on the model's performance. Our findings thus suggest that the ANOVA-F test can significantly improve the model's performance. Table 19 provides a summary of

TABLE 18. Performance evaluation of 5, 10, 15, 20, 24, 48 persons on different DL classification models.

Model	Min. Val. L	Train Acc. (%)	Test Acc. (%)	Prec.	Recall	F1-score	Support	Execution Time (second)
5 Person								
ANN	0.2502	96.5	94	0.96	0.96	0.96	50	5.78
ResMLP	0.1263	100	98	0.95	0.94	0.94	50	10.04
CNN1D	0.1653	100	98	0.98	0.98	0.98	50	5.39
CNN2D	0.1261	100	98	0.98	0.98	0.98	50	4.44
CNN_BiLSTM	0.4074	96.0	92	0.98	0.98	0.98	50	22.96
BiLSTM	0.1819	99.5	96	0.94	0.94	0.94	50	21.34
Hybrid	0.2282	100	94	0.96	0.96	0.96	50	4.77
10 Person								
ANN	0.0794	97.75	98	0.97	0.97	0.97	100	3.88
ResMLP	0.1165	99.75	95	0.95	0.95	0.95	100	10.38
CNN1D	0.0808	100	97	0.97	0.97	0.97	100	3.15
CNN2D	0.0648	100	98	0.97	0.97	0.97	100	5.79
CNN_BiLSTM	0.2145	99.0	97	0.96	0.96	0.96	100	27.27
BiLSTM	0.0960	98.0	97	0.97	0.97	0.97	100	24.05
Hybrid	0.0332	99.25	100	1.00	1.00	1.00	100	8.807
15 Person								
ANN	0.2482	91.60	93.15	0.94	0.93	0.93	146	4.77
ResMLP	0.2498	98.11	93.15	0.93	0.92	0.92	146	9.12
CNN1D	0.2010	99.82	96.57	0.95	0.95	0.95	146	2.65
CNN2D	0.1661	100.0	97.94	0.97	0.97	0.97	146	30.07
CNN_BiLSTM	0.3117	95.20	93.83	0.95	0.94	0.94	146	7.12
BiLSTM	0.2193	96.91	95.89	0.95	0.95	0.95	146	24.31
Hybrid	0.2180	95.89	95.89	0.96	0.96	0.96	146	3.369
20 Person								
ANN	0.1223	95.19	96.61	0.95	0.94	0.94	177	7.36
ResMLP	0.1801	99.29	95.48	0.93	0.93	0.93	177	10.40
CNN1D	0.1415	99.85	95.48	0.94	0.93	0.93	177	4.18
CNN2D	0.1294	100.0	97.17	0.97	0.96	0.96	177	6.80
CNN_BiLSTM	0.2739	93.21	94.91	0.92	0.93	0.92	177	35.78
BiLSTM	0.1613	94.48	96.04	0.92	0.93	0.92	177	30.96
Hybrid	0.2390	93.35	92.09	0.93	0.93	0.92	177	4.0
24 Person (Database 1)								
ANN	0.3321	82.98	90.80	0.92	0.91	0.91	244	8.244
ResMLP	0.4204	97.44	89.93	0.92	0.91	0.91	244	10.69
CNN1D	0.2197	99.13	94.27	0.92	0.91	0.90	244	6.51
CNN2D	0.2665	100.0	94.70	0.95	0.94	0.94	244	10.39
CNN_BiLSTM	0.5883	88.52	87.11	0.86	0.84	0.85	244	44.14
BiLSTM	0.2558	91.93	93.40	0.93	0.92	0.92	244	41.45
Hybrid	0.3676	91.83	91.67	0.92	0.91	0.91	244	5.0
24 Person (Database 2)								
ANN	0.1927	86.27	94.47	0.95	0.94	0.94	217	7.04
ResMLP	0.2130	98.15	95.39	0.96	0.95	0.95	217	9.48
CNN1D	0.1143	99.65	95.85	0.96	0.96	0.96	217	3.04
CNN2D	0.0890	100.0	98.15	0.97	0.97	0.97	217	7.85
CNN_BiLSTM	0.2930	91.46	91.70	0.92	0.92	0.91	217	39.39
BiLSTM	0.2179	91.69	94.00	0.95	0.94	0.94	217	39.14
Hybrid	0.2059	93.19	94.93	0.93	0.93	0.92	217	5.2
48 Person (Combined Database)								
ANN	0.3413	81.76	89.80	0.91	0.89	0.89	461	7.50
ResMLP	0.3637	97.88	90.02	0.91	0.89	0.89	461	12.76
CNN1D	0.2363	98.48	93.05	0.93	0.92	0.92	461	5.30
CNN2D	0.2906	100.0	93.05	0.94	0.93	0.93	461	11.25
CNN_BiLSTM	0.6414	88.71	85.46	0.87	0.84	0.84	461	78.49
BiLSTM	0.2512	91.80	93.05	0.94	0.93	0.93	461	87.21
Hybrid	0.3456	89.52	90.23	0.91	0.90	0.90	461	5.5

TABLE 19. Comparison of our proposed method with other recent related studies.

References	Source type of Data	Dependency	Users	Data Type	Methods	Reported Accuracy (%)
Ref. [1]	Pen tablet sensor	Text-independent	25	English Text	SVM, LR, RF	98.0
Ref. [7]	Handwritten Pattern	Text-independent	57	Two patterns	SVM, RF	89.8
Ref. [8]	Pen tablet sensor	Text-independent	33	Kanji character	SVM	99.0
Ref. [18]	Image	Text-dependent	100	Devanagari characters	k-NN and linear SVM	91.53
Ref. [19]	Behavior/Action	Text-independent	36	English Text	KNN, RF	97.1
Ref. [22]	Image	Text-independent	105	Handwriting thickness descriptor (HTD)	DL, ResNet	88.95
Ref. [42]	Pen tablet sensor	Text-independent	20	English Text	SVM, RF	72.44
Our Proposed	Pen tablet sensor	Task dependent / independent	48	English Text	K-SVM, CATBOOST, LGBM (ML)	100.0
					BiLSTM, CNN2D, Hybrid (DL)	98.31

the comparisons between our proposed models and other relevant studies. Ultimately, a variety of models were used to experiment with this research, and the findings were outstanding, with a lower processing cost and an increased accuracy rate.

V. CONCLUSION AND FUTURE WORKS

In conclusion, this study introduces an advanced user identification system that analyses handwriting time series and real-time numeric data collected by a pen-tablet sensor. The promising results obtained from this system indicate its effectiveness in successfully identifying users. Two databases, each consisting of 24 samples from 48 users, were utilized to experiment. The research extracted 6-dimensional parameters, including pressure, time, X-axis, Y-axis, horizontal angle, and vertical angle, from the handwriting time-series data. Moreover, four features, such as statistical, kinematic, spatial, and composite, totalling 91 features, were extracted. Notably, the study identified 36 novel features from the 6-Dimensional time-series data, such as average pressure, velocity, horizontal angle, the vertical angle at starting position, ending position, peak height position, etc. These novel features significantly increased the system's efficiency compared to the existing system developed by previous researchers.

Four feature selection techniques (Pearson's r correlation, ANOVA F-test, Mutual Information gain, PCA) were experimented on the dataset to optimize the system's performance. Additionally, the experiment showed different angles and variations implemented on the data, such as taking 5/10/15/20/24/48 persons into account and individual task accuracy to prove the research's versatility.

Both ML and DL-based approaches were utilized, with the results showing that the system provides high accuracy ranging from 90.32%−96.32% and 93.44%−98.36% for the ML-based approach, without feature selection and for k-fold, respectively. In addition, the system provides high accuracy ranging from 91.0%−100.00% for individual words/tasks for high-performing algorithms, with feature selection. The DL-based approach demonstrated high efficiency ranging from 90.80%−94.70% without feature selection and 95.93%−96.93% for ANOVA-F selected feature and 93.32%−98.31% for PCA, whereas also showing a 94%−100% accuracy range in the case of individual tasks. Based on these results, we can conclude that the proposed system is highly robust and accurate in identifying users, with a near 100% accuracy rate. Furthermore, the proposed system can effectively classify handwriting datasets, making it suitable for real-world applications such as signature verification, forensic investigation, and mental state analysis. The system is also reliable in estimating the author with minimal computing resources and hardware expenditures, making it a suitable application for mobile devices with limited storage space. Overall, this study contributes to advancing user identification systems and presents a promising solution to real-world identification challenges.

Future Directions

The area of user identification based on handwriting fine motor data offers significant promise for future study and development. With technological advancements and the availability of bigger datasets, it is feasible to enhance the classification of many people and the identification of a broader spectrum of unusual diseases. One area of emphasis may be the use of deep learning models, which have shown considerable promise in a variety of other domains, to increase the accuracy of user identification utilizing handwriting fine motor data. These models might be trained on larger datasets, resulting in more robust and trustworthy outcomes. Including other motions beyond handwriting, such as hand movement and grip strength, to identify even more complicated circumstances might be an additional research topic; thus, This might result in the creation of a method of user identification that takes into consideration a wider range of physical and behavioral characteristics.

In conclusion, there is a great deal of space for expansion and study in the subject of user identification utilizing handwriting fine motor data, and researchers will probably continue to make major strides in the next years.

REFERENCES

[1] N. Begum, M. A. H. Akash, S. Rahman, J. Shin, M. R. Islam, and M. E. Islam, "User authentication based on handwriting analysis of pen-tablet sensor data using optimal feature selection model," *Future Internet*, vol. 13, no. 9, p. 231, Sep. 2021.

[2] J. Tian, C. Qu, W. Xu, and S. Wang, "KinWrite: Handwriting-based authentication using Kinect," in *Proc. NDSS*, vol. 93, 2013, p. 94.

[3] Y. Zhang, F. Monrose, and M. K. Reiter, "The security of modern password expiration: An algorithmic framework and empirical analysis," in *Proc. 17th ACM Conf. Comput. Commun. Security*, Oct. 2010, pp. 176–186.

[4] J. Cornwell, I. Fette, G. Hsieh, M. Prabaker, J. Rao, K. Tang, K. Vaniea, L. Bauer, L. Cranor, J. Hong, B. Mclaren, M. Reiter, and N. Sadeh, "User-controllable security and privacy for pervasive computing," in *Proc. 8th IEEE Workshop Mobile Comput. Syst. Appl.*, Mar. 2007, pp. 14–19.

[5] (2006). *NSTC Subcommittee on Biometrics, Privacy & Biometrics Building a Conceptual Foundation*. [Online]. Available: www.biometricscatalog.org/NSTCSubcommittee

[6] J. Shin, M. A. M. Hasan, M. Maniruzzaman, A. Megumi, A. Suzuki, and A. Yasumura, "Online handwriting based adult and child classification using machine learning techniques," in *Proc. IEEE 5th Eurasian Conf. Educ. Innov. (ECEI)*, Feb. 2022, pp. 201–204.

[7] J. Shin, M. Maniruzzaman, Y. Uchida, M. A. M. Hasan, A. Megumi, A. Suzuki, and A. Yasumura, "Important features selection and classification of adult and child from handwriting using machine learning methods," *Appl. Sci.*, vol. 12, no. 10, p. 5256, May 2022.

[8] M. A. M. Hasan, J. Shin, and M. Maniruzzaman, "Online kanji characters based writer identification using sequential forward floating selection and support vector machine," *Appl. Sci.*, vol. 12, no. 20, p. 10249, Oct. 2022.

[9] S. Gupta, "Automatic person identification and verification using online handwriting," *Int. Inst. Inf. Technol.*, vol. 408, pp. 1–102, Mar. 2008.

[10] M. A. H. Akash, N. Begum, S. Rahman, J. Shin, M. Amiruzzaman, and M. R. Islam, "User authentication through pen tablet data using imputation and flatten function," in *Proc. 3rd IEEE Int. Conf. Knowl. Innov. Invention (ICKII)*, Aug. 2020, pp. 208–211.

[11] M. A. Emran, S. Naief, and M. S. Hossain, "Handwritten character recognition and prediction of age, gender and handedness using machine learning," Ph.D. dissertation, Dept. Comput. Sci. Eng. (CSE), BRAC Univ., Dhaka, Bangladesh, 2018.

[12] R. Plamondon and G. Lorette, "Automatic signature verification and writer identification—The state of the art," *Pattern Recognit.*, vol. 22, no. 2, pp. 107–131, Jan. 1989.

[13] P. Singhal, P. K. Srivastava, A. K. Tiwari, and R. K. Shukla, "A survey: Approaches to facial detection and recognition with machine learning techniques," in *Proc. 2nd Doctoral Symp. Comput. Intell. (DoSCI)*, Cham, Switzerland: Springer, Sep. 2022, pp. 103–125.

[14] R. G. Guimarães, R. L. Rosa, D. De Gaetano, D. Z. Rodríguez, and G. Bressan, "Age groups classification in social network using deep learning," *IEEE Access*, vol. 5, pp. 10805–10816, 2017.

[15] S. A. Maadeed and A. Hassaine, "Automatic prediction of age, gender, and nationality in offline handwriting," *EURASIP J. Image Video Process.*, vol. 2014, no. 1, pp. 1–10, Dec. 2014.

[16] Á. Morera, Á. Sánchez, J. F. Vélez, and A. B. Moreno, "Gender and handedness prediction from offline handwriting using convolutional neural networks," *Complexity*, vol. 2018, pp. 1–14, Jan. 2018.

[17] J. Shin and T. Okuyama, "Detection of alcohol intoxication via online handwritten signature verification," *Pattern Recognit. Lett.*, vol. 35, pp. 101–104, Jan. 2014.

[18] U. Gupta, H. Bansal, and D. Joshi, "An improved sex-specific and age-dependent classification model for Parkinson's diagnosis using handwriting measurement," *Comput. Methods Programs Biomed.*, vol. 189, Jun. 2020, Art. no. 105305.

[19] S. Dargan, M. Kumar, A. Garg, and K. Thakur, "Writer identification system for pre-segmented offline handwritten devanagari characters using k-NN and SVM," *Soft Comput.*, vol. 24, no. 13, pp. 10111–10122, Jul. 2020.

[20] B. S. Saini, P. Singh, A. Nayyar, N. Kaur, K. S. Bhatia, S. El-Sappagh, and J.-W. Hu, "A three-step authentication model for mobile phone user using keystroke dynamics," *IEEE Access*, vol. 8, pp. 125909–125922, 2020.

[21] D. Chen, Z. Ding, C. Yan, and M. Wang, "A behavioral authentication method for mobile based on browsing behaviors," *IEEE/CAA J. Autom. Sinica*, vol. 7, no. 6, pp. 1528–1541, Nov. 2020.

[22] H. T. Nguyen, C. T. Nguyen, T. Ino, B. Indurkhya, and M. Nakagawa, "Text-independent writer identification using convolutional neural network," *Pattern Recognit. Lett.*, vol. 121, pp. 104–112, Apr. 2019.

[23] M. Javidi and M. Jampour, "A deep learning framework for text-independent writer identification," *Eng. Appl. Artif. Intell.*, vol. 95, Oct. 2020, Art. no. 103912.

[24] A. Rehman, S. Naz, M. I. Razzak, and I. A. Hameed, "Automatic visual features for writer identification: A deep learning approach," *IEEE Access*, vol. 7, pp. 17149–17157, 2019.

[25] A. Baldominos, Y. Saez, and P. Isasi, "A survey of handwritten character recognition with MNIST and EMNIST," *Appl. Sci.*, vol. 9, no. 15, p. 3169, Aug. 2019.

[26] L. Li, X. Zhao, and G. Xue, "Unobservable re-authentication for smartphones," in *Proc. NDSS*, vol. 56, 2013, pp. 57–59.

[27] N. Sae-Bae, N. Memon, K. Isbister, and K. Ahmed, "Multitouch gesture-based authentication," *IEEE Trans. Inf. Forensics Security*, vol. 9, no. 4, pp. 568–582, Apr. 2014.

[28] J. Fierrez, A. Pozo, M. Martinez-Diaz, J. Galbally, and A. Morales, "Benchmarking touchscreen biometrics for mobile authentication," *IEEE Trans. Inf. Forensics Security*, vol. 13, no. 11, pp. 2720–2733, Nov. 2018.

[29] K. Saranya and M. Vijaya, "Text dependent writer identification using support vector machine," *Int. J. Comput. Appl.*, vol. 65, no. 2, pp. 6–11, Jan. 2013.

[30] T. T, V. Ms, and K. S, "Analysis of Tamil character writings and identification of writer using support vector machine," in *Proc. IEEE Int. Conf. Adv. Commun. Control Comput. Technol.*, May 2014, pp. 1407–1411.

[31] Y. Nakamura and M. Kidode, "Individuality analysis of online kanji handwriting," in *Proc. 8th Int. Conf. Document Anal. Recognit. (ICDAR)*, 2005, pp. 620–624.

[32] A. Soma and M. Arai, "Writer identification for offline handwritten kanji without using character recognition features," in *Proc. Int. Conf. Inf. Sci. Technol. Appl.*, 2013, pp. 96–98.

[33] A. Semma, Y. Hannad, I. Siddiqi, C. Djeddi, and M. E. Y. El Kettani, "Writer identification using deep learning with FAST keypoints and Harris corner detector," *Expert Syst. Appl.*, vol. 184, Dec. 2021, Art. no. 115473.

[34] U.-V. Marti, R. Messerli, and H. Bunke, "Writer identification using text line based features," in *Proc. 6th Int. Conf. Document Anal. Recognit.*, 2001, pp. 101–105.

[35] R. Plamondon and S. N. Srihari, "Online and off-line handwriting recognition: A comprehensive survey," *IEEE Trans. Pattern Anal. Mach. Intell.*, vol. 22, no. 1, pp. 63–84, Jan. 2000.

[36] S. Madhvanath and V. Govindaraju, "The role of holistic paradigms in handwritten word recognition," *IEEE Trans. Pattern Anal. Mach. Intell.*, vol. 23, no. 2, pp. 149–164, Feb. 2001.

[37] J. Park, V. Govindaraju, and S. N. Srihari, "OCR in a hierarchical feature space," *IEEE Trans. Pattern Anal. Mach. Intell.*, vol. 22, no. 4, pp. 400–407, Apr. 2000.

[38] J. Patvarczki, A. Kornafeld, and E. Tamas, "Method for image-based authentication," U.S. Patent 12 753 225, Jan. 5, 2012.

[39] M. Moetesum, I. Siddiqi, N. Vincent, and F. Cloppet, "Assessing visual attributes of handwriting for prediction of neurological disorders—A case study on Parkinson's disease," *Pattern Recognit. Lett.*, vol. 121, pp. 19–27, Apr. 2019.

[40] J. Mucha, V. Zvoncak, Z. Galaz, M. Faundez-Zanuy, J. Mekyska, T. Kiska, Z. Smekal, L. Brabenec, I. Rektorova, and K. Lopez-de-Ipina, "Fractional derivatives of online handwriting: A new approach of parkinsonic dysgraphia analysis," in *Proc. 41st Int. Conf. Telecommun. Signal Process. (TSP)*, Jul. 2018, pp. 1–4.

[41] D. Impedovo, G. Pirlo, and G. Vessio, "Dynamic handwriting analysis for supporting earlier Parkinson's disease diagnosis," *Information*, vol. 9, no. 10, p. 247, Oct. 2018.

[42] G. Vessio, "Dynamic handwriting analysis for neurodegenerative disease assessment: A literary review," *Appl. Sci.*, vol. 9, no. 21, p. 4666, Nov. 2019.
[43] S. Akhtar, M. M. Dipti, T. A. Tinni, P. Khan, R. Kabir, and M. R. Islam, "Analysis on handwriting using pen-tablet for identification of person and handedness," in *Proc. Int. Conf. Inf. Commun. Technol. Sustain. Develop. (ICICT4SD)*, Feb. 2021, pp. 120–124.
[44] T. Onose, K.-S. Yun, and J. Shin, "Feature analysis of characters for signature evaluation," in *Proc. 3rd Int. Conf. Frontiers Inf. Technol., Appl. Tools (FITAT)*, Yanji, China, Jun. 2010, pp. 43–52.
[45] S. P. Deore and A. Pravin, "On-line devanagari handwritten character recognition using moments features," in *Proc. Int. Conf. Recent Trends Image Process. Pattern Recognit. (RTIP2R)*, Solapur, India. Cham, Switzerland: Springer, Dec. 2018, pp. 37–48.
[46] M. Andrew, D. Preston, J. Wolfe, and S. Yu, *Basic Statistics-Mean, Median, Average, Standard Deviation, Z-Scores, P-Value*. Ann Arbor, Michigan. Univ. Michigan, 2009. [Online]. Available: https://bit.ly/Basic_statistics
[47] Wikipedia. (2019). *Quartile*. [Online]. Available: https://en.wikipedia.org/wiki/Quartile
[48] M. Faundez-Zanuy, J. Fierrez, M. A. Ferrer, M. Diaz, R. Tolosana, and R. Plamondon, "Handwriting biometrics: Applications and future trends in e-Security and e-Health," *Cognit. Comput.*, vol. 12, no. 5, pp. 940–953, Sep. 2020.
[49] (2022). *Handwriting-Features: Module for the Computation of the Conventionally Used Handwriting Features From Online Handwriting With an Interface for the Featurizer API*. [Online]. Available: https://github.com/BDALab/handwriting-features
[50] J. Cai, J. Luo, S. Wang, and S. Yang, "Feature selection in machine learning: A new perspective," *Neurocomputing*, vol. 300, pp. 70–79, Jul. 2018.
[51] V. W. Berninger, "Coordinating transcription and text generation in working memory during composing: Automatic and constructive processes," *Learn. Disab. Quart.*, vol. 22, no. 2, pp. 99–112, May 1999.
[52] D. G. Bonett and T. A. Wright, "Sample size requirements for estimating Pearson, Kendall and Spearman correlations," *Psychometrika*, vol. 65, no. 1, pp. 23–28, Mar. 2000.
[53] P. Bobko, *Correlation and Regression: Applications for Industrial Organizational Psychology and Management*. Thousand Oaks, CA, USA: Sage Publications, 2001.
[54] J. Hartung, K. H. Makambi, and D. Argaç, "An extended ANOVA F-test with applications to the heterogeneity problem in meta-analysis," *Biometrical J.*, vol. 43, no. 2, pp. 135–146, May 2001.
[55] H. Alaskar, A. J. Hussain, W. Khan, H. Tawfik, P. Trevorrow, P. Liatsis, and Z. Sbaï, "A data science approach for reliable classification of neurodegenerative diseases using gait patterns," *J. Reliable Intell. Environ.*, vol. 6, no. 4, pp. 233–247, Dec. 2020.
[56] D. J. MacKay, *Information Theory, Inference and Learning Algorithms*. Cambridge, U.K.: Cambridge Univ. Press, 2003.
[57] (2023). *Support Vector Machine (SVM) Algorithm*. [Online]. Available: https://www.javatpoint.com/machine-learning-support-vector-machine-algorithm
[58] (2023). *Support Vector Machine*. [Online]. Available: https://en.wikipedia.org/wiki/Support_vector_machine
[59] Y. Y. Song and Y. Lu, "Decision tree methods: Applications for classification and prediction," *Shanghai Arch. Psychiatry*, vol. 27, no. 2, p. 130, Apr. 2015.
[60] B. John. *When to Choose CatBoost Over XGBoost or LightGBM [Practical Guide]*. Accessed: Feb. 19, 2023. [Online]. Available: https://neptune.ai/blog/when-to-choose-catboost-over-xgboost-or-lightgbm
[61] C. T. Tchakoute and K. L. Sainani, "Dealing with binary repeated measures data," *PM R J. Injury Function Rehabil.* vol. 10, no. 12, pp. 1412–1416, Dec. 2018.
[62] M. A. M. Hasan, M. Nasser, S. Ahmad, and K. I. Molla, "Feature selection for intrusion detection using random forest," *J. Inf. Secur.*, vol. 7, no. 3, pp. 129–140, 2016.
[63] Q. Xiao, X. Zhong, and C. Zhong, "Application research of KNN algorithm based on clustering in big data talent demand information classification," *Int. J. Pattern Recognit. Artif. Intell.*, vol. 34, no. 6, Jun. 2020, Art. no. 2050015.
[64] A. McCallum and K. Nigam, "A comparison of event models for naive Bayes text classification," in *Proc. AAAI Workshop Learn. Text Categorization*, vol. 752, no. 1, pp. 41–48, 1998.
[65] L. Bottou, "Large-scale machine learning with stochastic gradient descent," in *Proc. 19th Int. Conf. Comput. Statist.*, Paris, France, Aug. 2010, pp. 177–186.
[66] I. Goodfellow, Y. Bengio, and A. Courville, *Deep Learning*. Cambridge, MA, USA: MIT Press, 2016.
[67] H. Touvron, P. Bojanowski, M. Caron, M. Cord, A. El-Nouby, E. Grave, G. Izacard, A. Joulin, G. Synnaeve, J. Verbeek, and H. Jégou, "ResMLP: Feedforward networks for image classification with data-efficient training," *IEEE Trans. Pattern Anal. Mach. Intell.*, vol. 45, no. 4, pp. 5314–5321, Apr. 2023.
[68] R. Atienza, *LSTM by Example Using Tensorflow*. Accessed: Feb. 19, 2023. [Online]. Available: https://towardsdatascience.com/lstm-by-example-using-tensorflow-feb0c1968537

TAHMID HASAN received the Bachelor of Science (Engineering) degree in computer science and engineering from the Pabna University of Science and Technology, Pabna, Bangladesh, in 2023. He is currently working as a Research Assistance in Pattern Processing Lab, Department of Computer Science and Engineering, Pabna University of Science and Technology. His research interests include pattern processing, user authentication, natural language processing, human–computer interaction, and computer vision.

MD. ABDUR RAHIM received the Bachelor of Science (Hons.) and Master of Science (M.Sc.) degrees in computer science and engineering from the University of Rajshahi, Bangladesh, in 2008 and 2009, respectively, and the Ph.D. degree from the Graduate School of Computer Science and Engineering, The University of Aizu, Fukushima, Japan, in 2020. He is currently an Associate Professor and the Head of the Department of Computer Science and Engineering, Pabna University of Science and Technology, Pabna, Bangladesh. His research interests include human–computer interaction, pattern recognition, computer vision and image processing, human gesture recognition, non-touch interfaces, machine intelligence, and handwriting analysis, recognition, and synthesis. He has several publications in major journals (SCI and SCIE-indexed) and conferences. He also serves as a reviewer for several SCI and SCIE-indexed journals and international conferences.

JUNGPIL SHIN (Senior Member, IEEE) received the B.Sc. degree in computer science and statistics and the M.Sc. degree in computer science from Pusan National University, South Korea, in 1990 and 1994, respectively, and the Ph.D. degree in computer science and communication engineering from Kyushu University, Japan, in 1999, under a scholarship from the Japanese Government (MEXT). He was an Associate Professor, a Senior Associate Professor, and a Full Professor with the School of Computer Science and Engineering, The University of Aizu, Japan, in 1999, 2004, and 2019, respectively. He has coauthored more than 350 published papers for widely cited journals and conferences. His research interests include pattern recognition, image processing, computer vision,

machine learning, human–computer interaction, nontouch interfaces, human gesture recognition, automatic control, Parkinson's disease diagnosis, ADHD diagnosis, user authentication, machine intelligence, bioinformatics, and handwriting analysis, recognition, and synthesis. He is a member of ACM, IEICE, IPSJ, KISS, and KIPS. He served as the program chair and as a program committee member for numerous international conferences. He serves as an Editor for IEEE journals, Springer, Sage, Taylor and Francis, *Sensors* (MDPI), *Electronics* (MDPI), and Tech Science. He serves as an Editorial Board Member for *Scientific Reports*. He serves as a reviewer for several major IEEE and SCI journals.

SATOSHI NISHIMURA (Member, IEEE) received the B.E. degree from Tohoku University, in 1987, and the M.Sc. and D.Sc. degrees in information science from The University of Tokyo, in 1989 and 1995, respectively. He is currently a Senior Associate Professor with The University of Aizu. His research interests include computer graphics and computer music. He is a member of ACM and IPSJ.

MD. NAJMUL HOSSAIN (Member, IEEE) was born in Rajshahi, Bangladesh, in 1984. He received the B.Sc. and M.Sc. degrees in applied physics and electronic engineering (presently named as, electrical and electronic engineering) from the University of Rajshahi, Rajshahi, in 2007 and 2008, respectively, and the Ph.D. degree in the field of advanced wireless communication systems from the Graduate School of Science and Engineering, Saitama University, Saitama, Japan, in 2020. He is currently an Associate Professor with the Department of Electrical, Electronic and Communication Engineering, Pabna University of Science and Technology, Pabna, Bangladesh. He is collaboratively doing his research with several renowned professors, such as Prof. Tetsuya Shimamura, Saitama University, Japan; Prof. Jungpil Shin, The University of Aizu, Japan; and Prof. Heung-Gyoon Ryu's Commlab, Chungbuk National University, South Korea. His current research interests include electronics, antenna and wave propagation, wireless communications, and corresponding signal processing, especially for OFDM, orthogonal time frequency space (OTFS), orthogonal chirp division multiplexing (OCDM), MIMO, and future-generation wireless communication networks. He received the Gold Medal for his excellent academic performance.